Title
Slow phosphorylation of a tyrosine residue in LAT optimizes T cell ligand discrimination

Journal
Nature Immunology, 20(11)

ISSN
1529-2908

Authors
Lo, Wan-Lin
Shah, Neel H
Rubin, Sara A
et al.

Publication Date
2019-11-01

DOI
10.1038/s41590-019-0502-2

Peer reviewed

HHS Public Access

Author manuscript

Nat Immunol. Author manuscript; available in PMC 2020 April 14.

Published in final edited form as:

Nat Immunol. 2019 November ; 20(11): 1481–1493. doi:10.1038/s41590-019-0502-2.

Slow phosphorylation of a tyrosine residue in LAT optimizes T cell ligand discrimination

Wan-Lin Lo[1], **Neel H. Shah**[2,10], **Sara A. Rubin**[3,4], **Weiguo Zhang**[5], **Veronika Horkova**[6], **Ian R. Fallahee**[2], **Ondrej Stepanek**[6], **Leonard I. Zon**[3,4,7], **John Kuriyan**[2,8], **Arthur Weiss**[1,9,*]

[1]Division of Rheumatology, Rosalind Russell and Ephraim P. Engleman Arthritis Research Center, Department of Medicine, University of California, San Francisco, San Francisco, CA 94143, USA.

[2]Departments of Molecular and Cell Biology, University of California, Berkeley, Berkeley, CA 94720, USA.

[3]Harvard Stem Cell Institute, Harvard University, Cambridge, MA 02138, USA.

[4]Stem Cell Program and Division of Hematology/Oncology, Boston Children's Hospital and Dana-Farber Cancer Institute; Program in Immunology, Harvard Medical School, Boston, MA 02115, USA.

[5]Department of Immunology, Duke University Medical Center, Durham, NC 27710, USA.

[6]Institute of Molecular Genetics of the Czech Academy of Sciences, 142 20 Prague, Czech Republic.

[7]Howard Hughes Medical Institute, Boston Children's Hospital and Harvard University, Boston, MA 02115, USA.

[8]Howard Hughes Medical Institute, University of California, Berkeley, Berkeley, CA 94720, USA.

[9]Howard Hughes Medical Institute, University of California, San Francisco, San Francisco, CA 94143, USA.

[10]Current Address: Department of Chemistry, Columbia University, New York, NY 10027, USA.

Abstract

Self/non-self discrimination is central to T cell-mediated immunity. The kinetic proofreading model can explain T cell antigen receptor (TCR) ligand discrimination; however, the rate-limiting steps have not been identified. Here, we show that tyrosine phosphorylation of the T cell adaptor protein LAT at position Y132 is a critical kinetic bottleneck for ligand discrimination. LAT phosphorylation at Y132, mediated by the kinase ZAP-70, leads to the recruitment and activation

*Correspondence: art.weiss@ucsf.edu.

AUTHOR CONTRIBUTIONS

Conceptualization, W-L.L, N.H.S., J.K. and A.W; Methodology, W-L.L, N.H.S., S.A.R., L.I.Z., J.K. and A.W.; Investigation, W-L.L, N.H.S, S.A.R., and I.R.F.; Writing – Original Draft, W-L.L, N.H.S., S.A.R. and A.W.; Writing – Review & Editing: W-L.L, N.H.S., S.A.R., V.H., I.R.F.,W.Z., O.S., L.I.Z., J.K. and A.W.; Resources, W.Z., V.H. and O.S.; Supervision, L.I.Z., J.K. and A.W.; Funding Acquisition, W-L.L, N.H.S., W.Z., O.S., L.I.Z., J.K. and A.W.

COMPETING INTERESTS STATEMENT

The authors declare no competing financial interests.

of phospholipase C-γ1 (PLC-γ1), an important effector molecule for T cell activation. The slow phosphorylation of Y132, relative to other phosphosites on LAT, was governed by a preceding glycine residue (G131) but could be accelerated by substituting this glycine with aspartate or glutamate. Acceleration of Y132 phosphorylation increased the speed and magnitude of PLC-γ1 activation and enhanced T cell sensitivity to weaker stimuli, including weak agonists and self-peptides. These observations suggest that the slow phosphorylation of Y132 acts as a proofreading step to facilitate T cell ligand discrimination.

INTRODUCTION

T cell responses, mediated by T cell antigen receptors (TCRs), are remarkable for their high sensitivity, exquisite specificity, and rapidity[1]. T cells can be activated in response to very few foreign peptide-major histocompatibility complex (pMHC) ligands (one to ten)[2–4], with a small error rate (10^{-4} to 10^{-6})[5, 6] and rapid response time (seconds to a few minutes)[7]. This rapid and highly accurate responsiveness allows T cells to detect peptides derived from foreign pathogens or abnormal cells early and efficiently without reacting to self-tissues. Several factors have been proposed to affect T cell discrimination and correlate with responsiveness, including the subtle differences in TCR-pMHC off-rates, on-rates, affinities and catch-bond formation. However, differences in these factors for agonist and non-agonist ligands are not always sufficient to explain the actual T cell error rate[8, 9].

The remarkable selectivity of T cells may be explained by a kinetic proofreading model[3, 6]. Following ligand binding, TCR-proximal signaling molecules undergo a series of biochemical reactions, such as phosphorylation, and these multiple steps create a time delay between the input signal (pMHC recognition) and the output response (T cell activation)[6]. If these signaling steps are rapidly reversible upon removal of the stimulus (*e.g.*, through dephosphorylation by phosphatases), the TCR:pMHC interaction would have to persist for a sufficient duration to initiate successful activation. By this mechanism, small differences in TCR:pMHC affinities or off-rates could lead to vastly different cellular outcomes, with each signaling step functioning as a “proofreader” to allow only a bona-fide activation signal to propagate downstream. Thus far, most efforts to assess the importance of kinetic proofreading in TCR signaling have been restricted to biochemical or mathematical models, and have failed to account for the role of endogenous self-peptides and the changes of ligand discrimination during development[1, 10, 11].

LAT, the Linker for Activation of T cells, is an important scaffold that coordinates TCR proximal signals in a phosphorylation-dependent manner following receptor stimulation[12, 13]. Although there are several phosphorylation sites in LAT that play a role in signal transduction, Y132 is the only residue in LAT that recruits PLC-γ1 upon its phosphorylation by ZAP-70. Binding of PLC-γ1 to phosphorylated-Y132 (p-Y132) in LAT leads to the Tec family kinase ITK-mediated PLC-γ1 phosphorylation and activation[14]. This activation of PLC-γ1 ultimately leads to calcium mobilization, ERK and protein kinase C (PKC) activation, and eventually cellular effector and transcriptional responses[12]. Interestingly, despite the importance of LAT p-Y132, the presence of a glycine at position 131 in LAT makes Y132 a particularly poor substrate for ZAP-70 because the kinase domain

of ZAP-70 strongly favors an acidic residue, aspartate or glutamate, at the -1 position relative to substrate tyrosine residues[15].

Here, we show that substitution of the glycine residue at the −1 position with aspartate or glutamate markedly increased the phosphorylation rate of LAT Y132 in T cells. This focused amino acid substitution in a signaling scaffold protein was sufficient to enhance T cell responsiveness to weak antigens/self-peptides. We demonstrated that slow phosphorylation of Y132 in LAT serves as an essential rate-limiting step in TCR signaling to enable ligand discrimination. Although a glycine at position 131 in LAT is highly conserved in tetrapods, some fish have other residues preceding the homologous tyrosine residue, including aspartate and glutamate that are more optimal for phosphorylation by ZAP-70. Our results point to the slow phosphorylation of LAT Y132 as an important regulatory mechanism that contributes to T cell ligand discrimination in most jawed vertebrates and might underlie the remarkable selectivity of T cells.

RESULTS

Mammalian LAT Y132 has a glycine at the −1 position, unlike other ZAP-70 substrates.

LAT and SLP-76 are two adaptors in T cells that rely on their phosphorylation by ZAP-70 to link initial TCR signals to many downstream cellular events required for full T cell activation (Fig. 1a)[12]. ZAP-70 has a strong preference for its substrate tyrosines to be surrounded by acidic residues, *i.e.*, aspartate and glutamate[15, 16]. These acidic residues facilitate substrate interaction with the ZAP-70 kinase domain, which is rich in basic residues in the substrate-binding region[15].

The marked preference for aspartate and glutamate at the −1 position in ZAP-70 substrates is reflected in almost all reported substrates of human ZAP-70, except for the Y132 in LAT (Fig. 1b). Human LAT Y132 has an unusually-placed small, neutral glycine residue (G131) at the −1 position (Fig. 1b), making Y132 a potentially poor substrate for ZAP-70. In support of this view, Y132 phosphorylation is delayed compared to the distal tyrosines on LAT and is coincident with PLC-γ1 phosphorylation[17]. This uniquely positioned glycine preceding LAT Y132 is observed at the homologous position in virtually all 68 mammalian species examined (Fig. 1c). Consistent with the distinct sequence features of the Y132 phosphosite, *in vitro* phosphorylation assays with the ZAP-70 kinase domain and the cytoplasmic region of LAT showed that LAT Y132 was phosphorylated by ZAP-70 with substantially slower kinetics relative to the rate of total tyrosine phosphorylation in LAT (Fig. 1d). Of note, mutation of Y127 to phenylalanine did not affect phosphorylation of Y132 in the *in vitro* kinase assay, arguing against a priming effect of this nearby site of phosphorylation.

To extend this analysis to cells, we used Csk-deficient Jurkat cells reconstituted with a PP1 analog-sensitive Csk mutant (J.CskAS), to rapidly activate Lck by inhibiting Csk-dependent phosphorylation of an inhibitory tyrosine in Lck (data not shown)[18]. Activated Lck could then phosphorylate TCR ITAMs and ZAP-70, allowing ZAP-70 to initiate its kinase activities in its native cellular environment without triggering the TCR. Such treatment showed slower tyrosine phosphorylation of Y132 than of Y171, and the phosphorylation of

PLC-γ1 exhibited similar time-dependent phosphorylation as Y132 (Supplementary Fig. 1a,b).

Scanning mutagenesis screens with LAT-derived peptides suggested that the substitution of G131 with virtually any other amino acid should enhance Y132 phosphorylation, with aspartate and glutamate substitutions showing the greatest enhancement (Supplementary Fig. 1c)[15]. In a colorimetric *in vitro* kinase assay, in which ATP consumption is coupled to NADH oxidation, the ZAP-70 kinase domain showed negligible activity toward a wild-type peptide encompassing Y132 (Fig. 1e,f). Replacement of the glycine at the −1 position with aspartate or glutamate greatly increased the phosphorylation efficiency of Y132 (Fig. 1e,f). Despite its slow phosphorylation by ZAP-70, LAT Y132 is a bona-fide well-established ZAP-70 substrate, as shown in the kinase assay (Fig. 1d), in the experiments where ZAP-70 deficiency but not Itk deficiency eliminated Y132 phosphorylation (Supplementary Fig. 1d), and as reported in the literature[19].

Since p-Y132 in LAT is directly upstream of PLC-γ1, we examined the possibility that the glycine at 131 might have been selected to promote a better PLC-γ1 interaction with the p-Y132 site. Phosphorylated Y132 interacts with the N-terminal SH2 domain of PLC-γ1[19, 20]. A peptide with glycine preceding Y132 exhibited comparable binding affinity to the PLC-γ1 N-SH2 domain as did a peptide with aspartate preceding Y132 (Supplementary Fig. 2a,b). A scanning mutagenesis screen for PLC-γ1 N-SH2 binding to LAT p-Y132 peptide mutants confirmed that most substitutions at G131 do not affect SH2 binding, whereas polar substitutions at V135 (the +3 position) in the p-Y132-containing peptide impaired SH2 binding, consistent with the known binding motif preference for PLC-γ1 N-SH2 (Supplementary Fig. 2c)[21]. It is also unlikely that the G131D/E mutations would change which kinase phosphorylates this site, because the D/E residue at the −1 position is disfavored by Src-family kinases and Tec-family kinases[15, 16]. Therefore, this highly conserved glycine at the −1 position impedes the efficiency of LAT Y132 phosphorylation by ZAP-70.

Mutation of LAT G131 to an aspartate or glutamate enhances calcium responses.

To determine how the glycine 131 preceding Y132 affects PLC-γ1-dependent signal transduction, *e.g.*, calcium responses, we substituted G131 with aspartate or glutamate in T cells. LAT and its G131 variants were used to reconstitute CRISPR/Cas9-generated LAT-deficient human Jurkat cells (J.LAT), hereafter termed J.LAT.WT, J.LAT.G131D, J.LAT.G131E. When these cells were stimulated with anti-CD3 mAb (OKT3), the G131D and G131E LAT variants markedly augmented the magnitude of maximal calcium peaks (Fig. 2a,b). Particularly evident at lower doses of anti-CD3, expression of G131D and G131E mutant LAT molecules endowed cells with faster and larger calcium responses than did wild-type LAT (Fig. 2a,c). Thus, by mutating G131 to an aspartate or glutamate, the reconstituted J.LAT cells became more sensitive and responded more rapidly to weak anti-CD3 stimuli.

We examined whether the elevated calcium mobilization in J.LAT.G131D and J.LAT.G131E cells resulted from alteration of LAT Y132 and PLC-γ1 phosphorylation. J.LAT.G131D and J.LAT.G131E cells responded to lower anti-CD3 concentrations than did wild-type cells

(Fig. 2d, Supplementary Fig. 3a). The mutation at G131 did not influence the activation of Lck and ZAP-70 (Supplementary Fig. 3a,b), yet LAT Y132 and PLC-γ1 phosphorylation were greatly enhanced in G131D- and G131E-expressing cells (Fig. 2d, Supplementary Fig. 3a,c). Notably, we sometimes observed an enhancement in the phosphorylation of the distal tyrosine residues in cells expressing LAT G131D, however this effect was not consistently observed (Fig. 2d, Supplementary Fig. 3b). In time-course experiments, G131D or G131E LAT also accelerated the phosphorylation of LAT Y132 and PLC-γ1 (Fig. 2e). These results suggest that LAT G131D and G131E lowered the TCR response threshold and amplified T cell responsiveness by promoting the phosphorylation of LAT Y132 and PLC-γ1.

Enhanced Y132-PLC-γ1-derived signals allow T cells to respond to low affinity ligands.

The OT-I TCR recognizes a peptide spanning residues 257–264 from chicken ovalbumin (OVA) presented by the H-2K^b MHC molecules. Substitutions of one or two amino acids convert the full agonist OVA peptide into partial or weak agonists, all termed “altered peptide ligands” (APLs), providing a sensitive and specific system to examine T cell ligand discrimination capability.

We reconstituted LAT-deficient OT-I$^+$hCD8$^+$ Jurkat cells with wild-type LAT or the G131D or G131E variants (termed J.OT-I.LAT.WT, J.OT-I.LAT.G131D, J.OT-I.LAT.G131E, respectively). Each cell clone was stimulated with OVA APL-pulsed H-2K^b-expressing T2 cells (T2-K^b)[22]. Cells upregulated the activation marker CD69 in response to OVA stimulation but remained unresponsive towards an unrelated peptide VSV (Fig. 3a). When the cells were stimulated with OVA or partial agonists Q4R7 or T4, G131D- and G131E-LAT expressing J.OT-I$^+$ cells were approximately ten-fold more sensitive to the peptide stimulus. Q4H7 is a very weak agonist and only activated approximately 30% of the J.OT-I.LAT.WT cells, yet approximately 60% of J.OT-I.LAT.G131D and 50% of J.OT-I.LAT.G131E cells were able to respond to Q4H7, as measured by CD69 upregulation (Fig. 3a,b). Another weak OVA APL peptide, G4, did not stimulate J.OT-I.LAT.WT cells to upregulate CD69, but was able to activate about 40% of G131D-expressing J.OT-I$^+$ T cells and 20% of G131E-expressing cells (Fig. 3a,b). The responses to Q4H7 and G4 peptides are noteworthy because both peptides can promote positive selection of OT-I$^+$ T cells in fetal thymic organ cultures and, thus, are considered to have an affinity in the range of positively selecting self-peptides[23, 24].

G131D or G131E-expressing J.OT-I$^+$ cells were also weakly activated by the naturally occurring positively selecting self-peptide for OT-I TCR, Catnb (derived from β-catenin residues 329–336)[25], whereas wild-type LAT-expressing cells were not (Fig. 3a,b). We compared the potency of each OVA APL peptide and self-peptide Catnb using J.OT-I$^+$ G131D/E versus wild-type LAT-expressing cells (Table 1). Peptide potencies were quantified by calculating EC_{50} (half maximal responses) in the CD69 upregulation assays and normalizing these values to the percentage of maximal CD69 responses[26]. These results suggest that the augmented LAT Y132 phosphorylation disrupted the cells’ abilities to accurately discriminate ligands with different potencies. G131D-expressing cells exhibited a lower ligand responsiveness threshold than wild-type LAT expressing cells.

CD69 upregulation is a prominent feature of T cell activation, but its expression can also be induced by exposure to cytokines[27]. Thus, we examined TCR-induced proximal signals, including phosphorylation of ERK and calcium flux, in response to OVA APL or self-peptide stimulation of J.OT-I$^+$ cells expressing LAT variants. LAT.WT-, G131D- or G131E-expressing J.OT-I$^+$ cells were first “barcoded” by labeling them with different dilutions of CellTrace Violet. All three variants were pooled and incubated with various peptide-pulsed T2-K^b cells at 37°C for 5 minutes (Fig. 4a). Stimulation with the OVA peptide induced the phosphorylation of ERK in all three J.OT-I$^+$ cell variants, but stimulation with the control peptide VSV did not (Fig. 4b and Supplementary Fig. 4a,b). Across all OVA and the APL peptide stimuli, a substantially larger population of G131D-expressing J.OT-I$^+$ cells exhibited ERK phosphorylation than did G131E-expressing J.OT-I$^+$ cells; and, the wild-type-expressing J.OT-I$^+$ cells were the least responsive. Dose-response analyses of the phospho-ERK induction further supported the stronger responses of LAT G131D- or G131E-expressing J.OT-I$^+$ cells toward full or partial agonist stimuli (Fig. 4c). Moreover, approximately 20% of G131D-expressing J.OT-I cells and 15% of G131E-expressing cells acquired the ability to upregulate ERK phosphorylation following stimulation with the self-peptide Catnb, whereas wild-type-expressing J.OT-I cells were unresponsive (Fig. 4c).

Next, we utilized OVA or APL-loaded biotinylated pMHC monomers and streptavidin to analyze antigen-specific calcium responses. Expression of G131D or G131E LAT augmented the calcium mobilization (Fig. 4d), enabling a more rapid, and 1.5- to 2-fold increases in the magnitude of the peak responses (Fig. 4e,f). Thus, a negatively charged residue preceding Y132 in LAT enhances a T cell’s ability to be more sensitive to full or partial agonist stimuli, and bestowed upon T cells the ability to respond, albeit weakly, to self-peptide stimulation.

Murine T cells rely on slow phosphorylation kinetics of Y136 in LAT to allow self/non-self antigen discrimination.

The mutations at LAT residue 131 elicited comparable functional consequences in primary mouse T cells. Ectopic over-expression of the G135D mutant LAT (Y136 is the murine ortholog of human Y132) in the presence of endogenous LAT was sufficient to endow OT-I$^+$ CD8 and OT-II$^+$ CD4 T cells with a gain-of-function ability to respond to low-affinity ligands (Supplementary Fig. 5). OT-I$^+$ CD8 or OT-II$^+$ CD4 T cells transduced with a retrovirus encoding wild-type LAT-P2A-BFP or G135D LAT-P2A-BFP were stimulated with various peptide-pulsed T cell-deficient splenocytes. In response to stimulation with G4 peptide-pulsed splenocytes, the expression of G135D LAT enabled OT-I$^+$ CD8 T cells to increase the expression of the key transcriptional factor IRF4 and activation marker CD69 (Supplementary Fig. 5a), augment the activation of ERK phosphorylation (Supplementary Fig. 5b), and promote the mobilization of calcium (Supplementary Fig. 5c). Similar gain-of-function was observed in G135D LAT-expressing OT-II$^+$ CD4 T cells when stimulated with the E336Q peptide, a partial agonist of OVA peptide (residue 329–336) specific for OT-II$^+$ TCR (Supplementary Fig. 5a,b).

Our data suggested that the human G131-Y132 and the homologous mouse G135-Y136 LAT sequences may place an important regulatory constraint on TCR signaling that enables

ligand discrimination. To further test this hypothesis in the absence of endogenous LAT, we utilized a mouse expressing a floxed *Lat* allele in which germline *Lat* could be deleted by tamoxifen treatment[28]. Expression of endogenous, wild-type LAT is expressed during thymic selection in the CD8 lineage of ERCre^{+}OT-I^{+}*Lat*$^{f/-}$ mouse. We used wild-type or G131D-expressing lentivirus to transduce the peripheral ERCre^{+}OT-I^{+}LAT$^{f/-}$ CD8 T cells from these mice. Tamoxifen-treatment was then used *in vitro* to delete endogenous *Lat* in mature OT-I^{+} T cells, enabling experimental assessment of the function of the lentivirally expressed LAT mutant (Fig. 5a).

ERCre^{+}OT-I^{+}*Lat*$^{f/-}$ CD8 T cells transduced with wild-type or G135D-P2A-mCherry lentivirus showed similar transduction frequencies and expression (Fig. 5b). The P2A sequence allows the mCherry fluorescence to function as a marker for successful transduction[29] and its fluorescence intensity can serve as a surrogate marker for protein expression without interfering with LAT function. The mCherry^{+} ERCre^{+}OT-I^{+}*Lat*$^{f/-}$ CD8 T cells re-gained the ability to respond to OVA and the partial agonist Q4R7 stimulation, as shown by the upregulation of CD69, but the non-transduced mCherry-negative cells did not (Supplementary Fig. 6). Expression of the G135D LAT mutant lowered the reactivity threshold to allow for a greater percentage of cells to be activated compared with that of wild-type LAT. The difference was particularly noteworthy when cells were stimulated with low-affinity peptides, such as the G4 peptide or the natural self-peptide Catnb (Fig. 5c,d). A small but increased response to the VSV peptide-pulsed APCs was also seen in the LAT-G135D-expressing cells. This could reflect responses to endogenous self-peptides that the VSV-pulsed APCs also expressed. The percentages of IFN-γ-producing cells in G135D^{+} groups also increased compared with those in the wild-type groups (Fig. 5e,f). Thus, an aspartic acid preceding Y136 endowed mature T cells with the ability to be activated by low affinity antigens and allowed at least one relevant self-peptide to become an agonist. Our data suggest that ZAP-70 mediated phosphorylation of LAT Y136 in primary mouse T cells may function as a critically important node involved in kinetic proofreading to enforce T cell ligand discrimination.

T cell ligand discrimination is uniquely susceptible to the phosphorylation kinetics of LAT Y132

The kinetic proofreading model predicts that proper ligand discrimination can be achieved by a series of gated biochemical events. In addition to the proofreading node involving LAT Y132 as shown here, co-receptor scanning and delivery of Lck can also influence T cell ligand discrimination[26]. To experimentally compare the relative contributions of coreceptor scanning and those involving G131-Y132 of LAT in TCR signaling, we again employed the OT-I^{+} Jurkat cells and OVA-APL systems. We used OT-I^{+} LAT-deficient Jurkat cells that did or did not express human CD8, and ectopically expressed wild-type LAT or the G131D mutant (termed J.OT-I.hCD8neg.LAT.WT or J.OT-I.hCD8neg.LAT.G131D, respectively). With these cells, we performed experiments as we did in Fig. 3. The presence of hCD8 appeared to enhance the sensitivity of cells' responses toward OVA peptide or partial agonists Q4R7, T4, or Q4H7, compared with cells lacking hCD8, but did not alter the EC_{50} value of cells' responses toward the low-affinity peptide G4 or self-peptide Catnb (Supplementary Fig. 7b,c). Thus, G131-Y132 of LAT creates an important TCR signaling

bottleneck that is distinct from the previously-reported time delay generated by co-receptor scanning[26].

To investigate whether the slow phosphorylation of Y132 in LAT is a unique rate-limiting step to control ligand discrimination, we explored the possibility that any of the other four individual tyrosine residues in LAT (that are phosphorylated more efficiently than Y132) could comparably function as "artificial" TCR signaling bottlenecks to further improve T cell ligand discrimination. We expressed "GY series" LAT mutants in J.OT-I^{+}.hCD8^{+} LAT-deficient cells (termed J.OT-I.LAT.G126Y127, J.OT-I.LAT.G170Y171, J.OT-I.LAT.G190Y191, or J.OT-I.LAT.G225Y226, respectively). Interestingly, these mutants and wild-type LAT showed comparable CD69 expression levels after stimulation with OVA or partial agonists Q4R7 or T4-pulsed T2-K^{b} cells (Supplementary Fig. 7d). The artificial attenuation of phosphorylation at LAT tyrosines other than Y132 did not influence OT-I TCR sensitivity or specificity, albeit there is likely redundancy in binding interactions with other SH2-containing proteins at the other phosphorylation sites. Thus, T cell ligand discrimination is preferentially controlled by the slow phosphorylation of LAT Y132 and likely depends upon the importance of events downstream of PLC-γ1.

Divergence at the LAT Y132 phosphosite in fish lineages may reflect temperature sensitive signaling.

The slow phosphorylation kinetics of Y132 can be largely attributed to a −1 glycine residue, which cannot form critical interactions with a conserved lysine residue (K538) in the substrate-binding site of the ZAP-70 catalytic domain[15, 16]. K538 and other positively-charged residues in the ZAP-70 active site are conserved across all jawed vertebrates (Fig. 6a)[15], suggesting that the substrate binding mode of ZAP-70 is conserved in these organisms. The glycine residue at position 131 in LAT is also highly conserved across jawed vertebrates, consistent with a conserved regulatory role for slow LAT Y132 phosphorylation (Fig. 6b,c). Interestingly, a "better neighbor" preceding Y132, such as asparagine, aspartate, and glutamate, is present in some fish (Fig. 6b). Among the other key tyrosines in LAT that get phosphorylated, there is also a relative lack of sequence conservation at the −1 positions among fish (Fig. 6d). Throughout jawed vertebrate evolution, however, the preceding sequence is dominated by a negatively-charged residue and lacking in any positively-charged residue, consistent with those features preferred by ZAP-70 for tyrosine phosphorylation (Fig. 6d).

Given our data on the critical role of the slow kinetics of Y132 phosphorylation for T cell ligand discrimination, we wondered why G131 is not completely conserved in fish. Based on our data in mammalian T cells, the other three amino acids observed at position 131 in fish LAT sequences (aspartate, glutamate, and asparagine) should speed up the phosphorylation of Y132 and enhance calcium responses toward low concentrations of anti-CD3 stimuli (data for G131N not shown). Why would some fish tolerate faster phosphorylation of this tyrosine if it might impair ligand discrimination?

Fish have a more limited antigen receptor repertoire[30], and are also generally cold-blooded[31]. We considered the possibility that better Y132 phosphorylation kinetics might provide certain immune-fitness advantages for these fish, as their body temperatures are

likely lower than those of mammals. To test the effect of temperature on the T cell's ability to induce calcium mobilization, we compared mouse and zebrafish thymocytes. Zebrafish have a naturally occurring aspartate preceding the tyrosine residue in LAT that is homologous to human Y132 and mouse Y136 (Fig. 6b). We used zebrafish that carry an *lck:eGFP* transgene to harvest the zebrafish thymi and identify thymocytes (Fig. 7a). Since no monoclonal antibodies are currently available to stimulate zebrafish TCRs or CD3[32], we stimulated zebrafish or mouse thymocytes with concanavalin A (Con A), a plant lectin that depends upon TCR expression to induce calcium increases in Jurkat T cells[33, 34]. Interestingly, temperature change had little impact on Con A responses of Lck-GFP$^+$ zebrafish thymocytes (Fig. 7b). In contrast, mouse thymocytes, which have a glycine preceding Y136, did not respond to Con A stimulation at lower temperatures (Fig. 7c and Supplementary Fig 8). Importantly, when the cells were treated with ionomycin, zebrafish and mouse thymocytes exhibited comparable maximal calcium responses, although responses were delayed in mouse thymocytes incubated at lower concentration (Fig. 7c).

Next, we tested whether G131D-expressing Jurkat cells may gain the temperature resistance properties seen in zebrafish thymocytes. We used biotinylated OVA H-2K^b monomers followed by crosslinking with streptavidin to stimulate J.OT-I.LAT.WT or J.OT-I.G131D cells. Notably, J.OT-I.LAT.WT cells were more vulnerable to the change of temperature than J.OT-I.LAT.G131D cells (Fig. 8a,b). At room temperature, the crosslinking of OVA H2-K^b was unable to induce calcium flux in wild-type LAT-expressing cells, whereas the change of temperature had minimal impairment on G131D-expressing J.OT-I$^+$ cells. Next, we used immunoblots to examine LAT phosphorylation of J.OT-I.LAT.WT or J.OT-I.LAT.G131D cells stimulated with biotin-labeled OVA monomers, followed by streptavidin crosslinking, across different temperatures. Although wild-type LAT was phosphorylated in response to stimulation at temperatures close to 37°C, we could not detect the phosphorylation of Y132 at 25°C or 28°C (Fig. 8c). In contrast, at room temperature stimulation, we could detect phosphorylation at those LAT tyrosines that have aspartate at the −1 positions (Y171 or G131D-preceding Y132), albeit much weaker compared to the stimulation at 37°C (Fig. 8c). Interestingly, we also observed an increased in basal phosphorylation of LAT Y132 and that of PLC-γ1 Y783 in J.OT-I.LAT.G131D cells, compared with those in J.OT-I.LAT.WT cells (Fig. 8c). Since we did not observe a similar increase in basal phosphorylation of Y132 in experiments that utilized anti-CD3 as the stimulus, the increase in basal phosphorylation here could be due to the prelabeling of cells with biotinylated OVA monomers at room temperature. Our sequence analyses and comparison of temperature effects on calcium responses in mouse versus zebrafish thymocytes, or wild-type LAT versus G131D-expressing OT-I$^+$ Jurkat cells suggest that slow LAT Y132 phosphorylation has been selected for in most jawed vertebrate lineages, and is virtually fixed in tetrapods. Some fish species, such as zebrafish, appear to have evolved to have faster phosphorylation of Y132, which may be required to enable signaling at the range of water temperatures in which these animals live in the wild (Supplementary Fig 9).

DISCUSSION

The balance of T cell sensitivity and specificity requires TCR discrimination of agonist pMHC from self-MHC which can differ by as little as a factor of ten in their affinities for the

TCR[35]. The kinetic proofreading model proposes that signal accuracy can be achieved by accepting some tolerable time delay through a series of reversible biochemical modifications before the commitment step that triggers a response. Here, we have shown that LAT functions as a critical time-keeper through constraints placed by a single residue, G131, which attenuates ZAP-70-mediated phosphorylation of Y132. The phosphorylation of Y132 is critical for the recruitment, phosphorylation, and activation of PLC-γ1. The activation of PLC-γ1 is critical for the subsequent calcium increase and PKC and Ras activation, which mediate T cell cytokine production, proliferation and effector responses. The molecular time delay at LAT Y132 is necessary for proper self/non-self discrimination, and our observations support the importance of slow Y132 phosphorylation in TCR kinetic proofreading.

Mutating G131 to aspartate leads to faster phosphorylation kinetics for Y132 but with negative consequences for ligand discrimination. Y132 is unique among the LAT phosphorylation sites in its ability to influence ligand discrimination, most likely because it is the only phosphorylation site that directly recruits PLC-γ1. The other four phosphorylation sites in LAT all have a YXNX motif, consistent with Grb2 or Gads recruitment sites[17, 36, 37]. Mutation of Y171, Y191, or Y226 has a minimal effect on T cell development and maturation[38]. In contrast, replacement of the Y132 with phenylalanine disrupts thymic development[39, 40], and also leads to TCR-independent lymphoproliferation of T cells, suggesting PLC-γ1 signals may maintain “balanced” cell signaling to ensure an appropriate T cell response[39–42]. Thus, Y132 in LAT is a potentially unique and important bottleneck, to temporally regulate the recruitment of PLC-γ1, with the help from other tyrosine residues (probably through Gads–SLP-76 preassembly on LAT to stabilize the PLC-γ1 binding)[17, 38, 43, 44]. Although artificial attenuation of LAT phosphorylation at individual tyrosine residues other than Y132 did not influence signaling sensitivity, we might expect that combinations of −1 glycine substitutions at LAT Y171, Y191, or Y226 would perturb T cell sensitivity.

There may be several events involved in kinetic proofreading, each of which could contribute to the time-delay required for ligand discrimination[26, 45, 46]. Notably, our study has identified an important contributor to kinetic proofreading that might have actionable therapeutic implications by providing a means for enhancing T cell responses to weaker agonists against pathogens that elicit weak responses, or to weak agonist peptides displayed by tumors. A tradeoff, however, might be the possibility of auto-reactivity. Interestingly, the LAT G131D mutation has a stronger effect than the G131E mutation in all of our data. From previous studies[16], we speculate that a −1 aspartate residue is the optimal shape/charge to coordinate a series of lysine residues near the substrate-binding pocket. Extending the acidic side chain by an extra methyl group would slightly disrupt this geometry.

The presence of a glycine residue preceding human Y132 creates a very poor substrate for ZAP-70[15]. While some fish have those more optimal residues preceding their homologous site in LAT, it is striking that virtually all tetrapodal LAT molecules examined have a glycine at this position. This could be the result of a strong selective pressure that was more relaxed in fish. Interestingly, other tyrosines of LAT have been under strong selection pressure in tetrapods to become good ZAP-70 substrates. The G131-Y132 is the only position that has

become an evolutionarily conserved poor substrate for ZAP-70 in tetrapods, which might reflect the need for optimal ligand discrimination.

Why, then, have some fish not adopted this same strategy for ligand discrimination? One major difference between tetrapods and fish is the maintenance of their body temperatures. Mammals are warm-blooded, whereas fish are cold-blooded, and the temperature of amphibians and reptiles can vary greatly depending on the environment. Various enzymes, including kinases, are sensitive to the temperature[47, 48]. Thus, some fish may require a more optimal ZAP-70 substrate to phosphorylate their LAT Y132 homologous sequences in order to activate PLC-γ1 when in cold water. Zebrafish T cells have a rather limited TCR repertoire, and they are more cross-reactive to self-antigens than mammalian T cells[30]. This may be one strategy to compensate for their limited and self-cross-reactive TCR repertoire, yet allow for protective T cell immunity to foreign antigens[30]. This increased self-reactivity of the zebrafish T cells may be constrained by the prominence of regulatory T cells to prevent auto-reactivity. T and B cell-mediated adaptive immunity evolved approximately 500 million years ago, with the emergence of jawed vertebrates[49, 50]. Since then, different organisms may have adapted slight variations on this system, as our analyses suggest for LAT phosphorylation. More comparisons of the sequences and activities of T cell signaling molecules across the animal kingdom are likely to reveal new mechanisms for the control of T cell activation.

METHODS

Experimental models

Animals—The C57BL/6 mice were housed in the specific pathogen-free facilities at the University of California, San Francisco. The ERCre^{+}LAT$^{f/f}$.OT-I mice were maintained at Duke University. Mice were treated according to protocols that were approved by University of California, San Francisco veterinary committees, or by Duke University animal care ethics committee, and are in accordance with NIH guidelines. Both males and females, 6–12 weeks of ages, were used in the studies. Zebrafish were maintained in accordance with Boston Children's Hospital Institutional Animal Care and Use Committee protocols and in line with Animal Resources at Children's Hospital (ARCH) guidelines. Tg(*lck:eGFP*) was previously described[55]. Male and female zebrafish between 2 and 4 months post-fertilization were used in all studies.

Cell lines—The human leukemic Jurkat T cell line, or Jurkat variants with LAT deficiency, or ZAP-70 deficiency, or ITK deficiency, or T2-K^{b} cells were maintained in RPMI culture medium supplemented with 5% fetal bovine serum and 2 mM glutamine. For additional drug selection, LAT-deficient Jurkat variants that were reconstituted with wild-type LAT or various mutant LAT constructs were maintained in 0.5 mg/ml of the aminoglycoside geneticin (G418; Santa Cruz Biotech), the Csk-AS Jurkat variant was maintained in 10 μg/ml blasticidin (Thermo Fisher Scientific).

Antibodies

Antibodies are listed in Reporting Summary and Supplementary Note.

Sequence alignments and analysis

Sequences of LAT orthologs from various jawed vertebrates were identified as described previously[15]. Briefly, human LAT was used as a query sequence for an initial protein-protein BLAST search using the NCBI non-redundant protein database[56, 57]. This initial search yielded mostly mammalian sequences, as well as a few fish, amphibian, and reptile sequences that were annotated to be LAT orthologs. These non-mammalian LAT sequences were used as queries in subsequent BLAST searches. Putative orthologous tyrosine phosphosites were identified in the C-terminal ~100 amino acids of each LAT sequence based on two criteria: (1) they matched the SH2 binding motifs, and (2) they occurred in the order seen for known human and mouse LAT phosphosites. The sequences surrounding individual putative phosphosites across all orthologs were manually aligned, and this local alignment was visualized using the online tool WebLogo[58].

LAT sequences of fish, birds, reptiles, and mammals

The sequences are listed in Supplementary Table 1.

Protein expression and purification, and *In vitro* phosphorylation assays

Please see Supplementary Note.

Generation of ZAP-70-deficient or ITK-deficient Jurkat variants

The ZAP-70-deficient or ITK-deficient Jurkat variants were generated by CRISPR/Cas9 technology as previously descripted[22]. In brief, guide sgRNAs that were against human *ZAP70*, or *ITK* coding regions were cloned into the pU6-(BbsI)_CBh-Cas9-T2A-BFP vector (Addgene Plasmid #64323), and electroporated into Jurkat T cells. The sgRNA sequences used in these studies were as follows: sgRNA nucleotide sequences against *ZAP70*: pair 1, 52-CACCGCATCGAGCAGGGCAAGCGGA-32 and 52-AAACTCCGCTTGCCCTGCTCGATGC-32; pair 2, 52-CACCGTTCGGGTGGACACTCTGGT-32 and 52-AAACACCAGAGTGTCCACCCGAAC-32. sgRNA nucleotide sequences against *ITK*: pair 1, 52-CACCGATACTTTGAAGATCGTCATG-32 and 52-AAACCATGACGATCTTCAAAGTATC-32; pair 2, 52-CACCGAAGCGGACTTTAAAGTTCGA-32 and 52-AAACTCGAACTTTAAAGTCCGCTTC-32.

Reconstituted LAT-deficient Jurkat with LAT mutants

LAT-deficient Jurkat cells were generated in our previous study[22] and was used for reconstitution with pEF-vectors that express wild-type LAT, G131D, or G131E mutants by electroporation..

Intracellular calcium measurements using a Flex Station

Calcium mobilization measured by a Flex Station II (Molecular Probes) was performed as previously described[22]. More details could be also found in the Supplementary Notes. In brief, 1×10^7 Jurkat variants were washed with PBS twice, and loaded with 1 μM Indo-1 AM calcium indicator dye (Thermo Fisher Scientific) individually at 37 °C for 30 min in 2

ml RPMI medium. 5×10^5 cells (100 μl) were washed twice again and transferred into individual wells in a flat-bottom 96-well plate. The temperature in Flex Station II was set to 37 °C and each plate was incubated in the Flex Station II for 5 min before the experiment was started. The cells were first left unstimulated for 30 sec to record basal levels of fluorescence intensities, followed by the addition of anti-CD3 (clone OKT3, Weiss lab) at the 30th sec and the addition of ionomycin (Thermo Fisher Scientific) at a later time point as specified in corresponding figure legends. Or, incubated with 1:100 dilution of OVA or APL-loaded biotinylated pMHC monomers (NIH Tetramer Core Facility) at 37 °C for 30 min in the pre-warmed Flex Station II. indo-1 fluorescence ratios were recorded for 30 sec to obtain the baseline relative calcium levels, followed by the addition of streptavidin (10 μg/ml; Jackson Immunoresearch) at the 30th sec and this was followed by the addition of ionomycin (Thermo Fisher Scientific) at the 240th sec. Data were imported into GraphPad Prism software for analysis and production of graphs.

Jurkat variants stimulated by concanavalin A (Con A) at different temperatures.—Jurkat variants were loaded with 1 μM of the Indo-1 calcium indicator dye at 25 °C for 30 min. After loading, cells were washed twice with PBS, and then resuspended in HBSS at a concentration of 5×10^6 cells per ml, and then transferred to a flat-bottom 96-well plate (5×10^6 cells per well) to record calcium-dependent fluorescence changes using the Flex Station II. The experiments started from a temperature of 25 °C which gradually increased throughout the experiments up to 37 °C. Each time, after the temperature of Flex Station II reached the pre-set temperature, the temperature was maintained for an extra few minutes before each experiment started. Con A was dissolved in ddH_2O at 10 μg/ml as a stock solution, which was further diluted in PBS to prepare 4× working solutions (120 μg/ml, 40 μg/ml, 12 μg/ml). The indo-1 fluorescence changes were recorded for 30 sec to obtain the baseline calcium level, followed by the addition of Con A at the 30th sec, and the calcium-dependent fluorescence changes were recorded for another 4.5 min. Data were imported into GraphPad Prism software for analysis and production of graphs.

Intracellular calcium measurements by flow cytometry

Mouse CD8 T cells stimulated by OVA or APL-loaded biotinylated pMHC monomers.—Naive OT-I$^+$ CD8 T cells were isolated and transduced with retrovirus expressing wild-type LAT-P2A-BFP or G135D LAT-P2A-BFP. Cells were loaded with 1 μM of the calcium-indicator dye Indo-1, 0.02% Pluronic F-127 (Thermo Fisher Scientific) at 37 °C in RPMI medium for 30 min, washed twice with PBS, and then labeled with 1:100 dilution of biotinylated OVA/H-2K^b, T4/H-2K^b, G4/H-2K^b, or VSV/H-2K^b monomers (NIH Tetramer Core Facility) at 37 °C for 30 min. Cells were then subject to flow cytometry-based calcium assays. Indo-1 cell associated fluorescence was first recorded for 30 sec to obtain a baseline and then monitored after additions. Streptavidin (10 μg/ml) was added at the 30th sec. Ionomycin was added at the 240th sec.

Zebrafish thymocytes stimulated by Con A at different temperatures.—Ice water immersion was used to euthanize the zebrafish before dissection of the thymi. Thymi were dissected from 15 or 16 zebrafish bilaterally into 800 μl of dissection solution: HBSS

(no Ca^{2+}, no Mg^{2+}) with 0.2% fetal bovine serum. After all of the thymi were collected, the solution was pipetted 15–20 times and filtered followed by filtration through a pre-moistened 40 μm cell strainer. Next, the cells were spun down at 400 × *g* for 5 min at 25 °C. The cell pellet was washed with 800 μl of dissection solution, spun down at 400 *g* for 5 min, and resuspended at 2.2×10^6 cells per ml in assay buffer (HBSS with Ca^{2+} and Mg^{2+}, 20 mM HEPES pH7.4). Indo 1-AM (Millipore Sigma) was pre-mixed 1:1 with Pluronic F-127 (Thermo Fisher Scientific) and added to the cell suspension at a final concentration of 1 μM Indo 1, 0.02% Pluronic F-127, and 0.18% DMSO and vortexed immediately. After incubating in the dark for 30 min at 28.5 °C, the cells were washed twice with assay buffer, spun down at 400 × *g* for 5 min at room temperature, and resuspended at a final concentration between 1.6×10^6 and 3.5×10^6 cells per ml in assay buffer. The cells were incubated at 15 °C, 25 °C, and 37 °C using Eppendorf thermomixers for 10–15 min prior to running on an LSRFortessa (BD Biosciences). Baseline calcium-dependent fluorescence was determined over a 30 second interval prior to the addition of stimulus: Con A (final concentration 10 μg/ml, Millipore Sigma) followed by the addition of ionomycin at the 240th sec to a final concentration of 1 μM.

Mouse thymocytes stimulated with Con A at different temperatures.—Thymi from C57BL/6 mice were harvested and prepared as single cell suspension in RPMI. Cells were labeled with 1 μM Indo-1 at 37 °C for 30 min, washed twice with PBS, and then resuspended in HBSS at the concentration of 1×10^7 cells per ml. The cells were incubated at 37 °C in a water bath, or at room temperature, or at 15 °C in a pre-cold benchtop centrifuge for at least 15 min before the experiment started. The calcium-dependent indo-1 fluorescence was recorded on an LSRFortessa (BD Biosciences,). The fluorescence was first recorded for 30 sec to obtain a baseline level, and then cells were stimulated with Con A at the 30th sec, followed the stimulation of ionomycin at the 240th sec. The Con A was purchased through the same vendor and lot number as the calcium experiments performed with zebrafish thymocytes.

Immunoblot analysis

Immunoblot analysis was performed as previously described[22] and more details could be found in the Supplementary Note.

CD69 activation assay

The J.OT-I.hCD8$^+$ or J.OT-I.hCD8neg series of Jurkat derivative cells expressing wild-type LAT or G131D, G131E variants were used in the experiments. A series of titrated concentrations of OVA or APL peptides was incubated with T2-K^b cells (2.5×10^5 cells per well) in flat-bottom 96-well plates at 37 °C for 1 h. 2.5×10^5 cells of J.OT-I$^+$hCD8$^+$ or J.OT-I$^+$hCD8neg series of Jurkat derivative cells were added into each well of the 96-well plate that contained the peptide-pulsed T2-K^b cells. The plates were incubated at 37 °C for ~16 h. For mouse OT-I$^+$ CD8 or OT-II$^+$ CD4 cells, cells were prepared and transduced to express wild-type or G135D LAT. Splenocytes from TCR Cα-deficient mice were used as antigen presenting cells. 5×10^5 cells per well of TCR Cα-deficient splenocytes were pulsed with titrated concentrations of OVA or APL peptides, and cultured with 5×10^5 cells of the

transduced mouse T cells at 37 °C for ~ 16 h. Upregulation of CD69 was analyzed on an LSRFortessa (BD Biosciences) the next day.

Phospho-ERK activation assay

T2-K^b cells (2.5×10^5 cells per well) were pulsed with titrated concentrations of OVA or APL peptides in U-bottom 96-well plates and incubated at 37 °C for 1 h. Individual clones of Jurkat derivative cells were barcoded by labeling each clone with differently titrated concentrations of CellTrace Violet (CTV: Thermo Fisher Scientific). Jurkat derivative cells expressing wild-type LAT were labeled with 2.5 μM CTV in PBS at 37 °C for 20 min in the dark, whereas G131D or G131E-expressing cells were labeled with 0.1 μM or 0.5 μM of CTV, respectively. Complete medium was then added to the cells for another 5 min of incubation at 37°C, and cells were washed with ice-cold PBS, and resuspended in PBS to the concentration of 2.5×10^6 cells per ml, and kept on ice. 2.5×10^5 cells of the barcoded Jurkat derivatives were added into each well that contained the peptide-pulsed T2-K^b cells. During the whole process the plates remained on ice. Cells were mixed well, and the plate was quickly centrifuged at 4 °C for 30 sec. The plate was then moved to a 37 °C water bath for 5 min to start the stimulation. The stimulation was stopped by the direct addition of 4% formaldehyde (final concentration to be 2%). The plate was incubated at 25 °C for 30 min for formaldehyde fixation. Cells were washed once with FACS buffer (2% FBS, 1 mM EDTA in PBS buffer), and permeabilized in 90% ice-cold methanol overnight at 4 °C. Cells were washed once with FACS buffer, rested in FACS buffer at 25 °C for 30 min, and stained with anti-phospho ERK (Cell Signaling Technology) for LSRFortessa analysis (BD Biosciences). For mouse T cells stimulated with OVA or APL pulsed Cα-deficient splenocytes, the procedures were similar to the experiments in Jurkat derivative cells, except that TCR Cα-deficient splenocytes were used as antigen-presenting cells.

IRF4 upregulation assay

Mouse OT-I^+ CD8 or OT-II^+ CD4 cells were prepared and transduced to express wild-type or G135D LAT. Cells were rested for one day before being used in the experiments. Splenocytes from Cα-deficient mice (2.5×10^5 cells per well) were mixed with titrated concentrations of OVA or APL peptides, mouse T cells, and incubated at 37 °C for ~ 16 h at 37 °C. Cells were washed once with FACS buffer (2% FBS, 1 mM EDTA in PBS buffer), and stained for CD4 or CD8, washed, and then fixed and permeabilized in Transcription Factor Staining Buffer (eBioscience/Thermo Fisher Scientific). Cells were stained with anti-IRF4 (BioLegend) and analyzed by LSRFortessa (BD Biosciences).

IFN-γ secretion assay

Mouse OT-I^+ CD8 or OT-II^+ CD4 cells were prepared and transduced to express wild-type or G135D LAT. A 48-well plate was coated with 1:100 dilution of OVA or APL-loaded biotinylated monomers the day before. Cells were washed and rested for one day in complete media without IL-2 before being used in the experiments. Cells were stimulated overnight at 37 °C and harvested for IFN-γ secretion analysis using IFN-γ Secretion Assay (Miltenyi Biotec,) and assessed by LSRFortessa (BD Biosciences).

Production of lentivirus or retrovirus expressing WT or G135D LAT

Murine WT-*Lat* was cloned into the pHR backbone under the expression of *Ef1a* promoter. Murine G135D-LAT mutant was generated using a QuickChange Lightning site-directed mutagenesis kit (Agilent Technologies). A C-terminal P2A self-cleaving peptide followed by mCherry was incorporated to assess transduction efficiency and expression levels. Packaging vector pCMV dR8.91, envelope vector pMD 2.G, and pHR.WT-LAT.P2A.mCherry or pHR.G135D-LAT.P2A.mCherry constructs were transiently co-transfected into LX-293T cells using TransIT-LT1 reagent (Mirus Bio). Supernatants containing virus particles were collected 48 h after transfection, filtered and concentrated by PEG 8000 precipitation. The virus particles were resuspended in PBS and stored at −80°C. For retrovirus-transduced experiments, murine WT-LAT or G135D-LAT were cloned into the pMSCV vectors individually, along with a C-terminal P2A self-cleaving peptide followed by BFP to help determine transduction efficiency and monitor expression level. Phoenix-Eco packaging cell line was transfected using Lipofectamine 2000 (Thermo Fisher Scientific). 48 h after transfection, the supernatants were harvested for experimental use. The viral supernatants were prepared freshly for each experiment.

Retroviral transduction of mouse peripheral CD8 or CD4 T cells

Naive mouse CD8 or CD4 T cells were isolated using biotinylated antibody cocktails (mix of anti-CD4 or CD8, together with anti-CD19, anti-B220, anti-CD11b, anti-CD11c, anti-DX5, anti-TER119, and anti-CD24) and magnetic beads-mediated negative selection (anti-biotin Miltenyi iBeads, Miltenyi Biotec). The retroviral supernatants (prepared freshly for every experiment) were first mixed with Lipofectamine (final concentration at 8 μg/ml) and IL-2 (final concentration at 50 U/ml), and incubated at 25 °C for 20–30 min. In a 24 well plate, 1×10^6 T cells were incubated with 1 ml retroviral supernatants/lipofectamine/IL-2 per well. The plate was wrapped in saran wrap and centrifuged at 460 × *g* for 1 h at 25 °C. The plate was then moved to a 37 °C incubator. BFP expression was monitored by LSRFortessa and can be seen 24 h after transduction (BD Biosciences).

Tamoxifen treatment and lentiviral transduction of mouse peripheral CD8$^+$ T cells

CD8$^+$ T cells from spleens of ERCre$^+$OT-I$^+$LAT$^{f/-}$ mice were prepared, and naive CD44^{lo}CD62L^{hi}Vα2$^+$ CD8$^+$ cells were sorted on FACSAria II (BD Biosciences). Naive CD8$^+$ T cells were cultured in a 24-well plate with 5 μg/ml plate-bound anti-CD3 (clone 2C11, Weiss lab) and 5 μg/ml soluble anti-CD28 (clone 37.51, Weiss lab) overnight at 37 °C. A non-tissue culture treated 24-well plate was coated with 3 μg RetroNectin (Takara Bio) in 250 μl PBS per well at 25 °C for 2 h, blocked with 2% BSA at 25 °C for 30 min, and then bound with concentrated lentivirus particles by centrifuging 460 × *g* for 1 h at 25 °C and washed with PBS. The next day, activated CD8$^+$ T cells were added to the RetroNectin-coated, lentivirus-bound plates and centrifuged at 460 × *g* for 5 min at 25 °C, and incubated at 37°C overnight in the presence of mouse IL-2 (10 ng/ml) and 50 nM 4-hydroxytamoxifen (Millipore Sigma) for 4 days. Tamoxifen-mediated deletion of endogenous LAT can be monitored by the expression of GFP, and the transduction efficiency can be monitored by the expression of mCherry. Cells were rested in the complete medium without IL-2 a day before being used in experiments.

Quantification and statistical analysis

Statistical analysis was applied to technical replicates, or biologically independent mice for each experiment. All experiments described in this study have been performed at least twice, and the exact numbers of independent experiments with similar results are indicated in the figure legends. All statistical analyses of experiments were performed using non-parametric, two-tailed Mann-Whitney tests. GraphPad Prism 6 Software (GraphPad Software) was used for data analysis and representation. All bar graphs show means with overlaid scatter dots, or error bars (indicating s.d.), to show the distribution of the data, as indicated in each figure legend. *P* values for comparisons are provided as exact values or as $P < 0.0001$ (exact values). 95% confident levels were used to determine a statistically significant *P* values.

Reporting Summary

Further information on experimental design is available in the Nature Research Reporting Summary linked to this article.

DATA AVAILABILITY STATEMENT

Further information and requests for resources and reagents should be directed to and will be fulfilled by the corresponding author, Arthur Weiss (art.weiss@ucsf.edu).

Supplementary Material

Refer to Web version on PubMed Central for supplementary material.

ACKNOWLEDGMENTS

We thank A. Roque (University of California, San Francisco) for animal husbandry; S. Muratcioglu (University of California, Berkeley) for providing the GFP-labeled PLC-γ1 tandem N-SH2 protein; NIH Tetramer Core Facility for providing the OVA and APL peptide loaded H-2K^b monomers or OVA loaded H-2A^b tetramers; UCSF Parnassus Flow Cytometry Core for maintaining the BD FACSAria II; R. Mathieu (Boston Children's Hospital) and BCH Department of Hematology/Oncology Flow Cytometry Research Facility for technical assistance; B. Au-Yeung (Emory University), P. Allen and D. Donermeyer (Washington University in St. Louis), G. Morris and L.-F. Lu (University of California, San Diego) for critical feedback on the manuscript. The work was supported by the Jane Coffin Childs Fund 61–1560 (to W.-L.L.), the Damon Runyon Cancer Research Foundation DRG 2198–14 & DFS 31–18 (to N.H.S.), the Czech Science Foundation 19–03435Y (to O.S.), the Howard Hughes Medical Institute (A.W. and J.K.) and NIH, NIAID P01 AI091580–06 (to A.W. and J.K.), 1R37AI114575 (to A.W.), and DRC Center Grant P30 DK063720 (UCSF Parnassus Flow Cytometry Core). All data to understand and access the conclusions of this study are available in the main text, the supplementary materials, and the indicated repositories.

REFERENCES

1. Feinerman O, Germain RN & Altan-Bonnet G Quantitative challenges in understanding ligand discrimination by alphabeta T cells. Mol. Immunol 45, 619–631 (2008). doi: 10.1016/j.molimm.2007.03.028. [PubMed: 17825415]
2. Brameshuber M et al. Monomeric TCRs drive T cell antigen recognition. Nat. Immunol 19, 487–496 (2018). doi: 10.1038/s41590-018-0092-4. [PubMed: 29662172]
3. Chakraborty AK & Weiss A Insights into the initiation of TCR signaling. Nat. Immunol 15, 798–807 (2014). doi: 10.1038/ni.2940. [PubMed: 25137454]
4. Huang J et al. A single peptide-major histocompatibility complex ligand triggers digital cytokine secretion in CD4(+) T cells. Immunity 39, 846–857 (2013). doi: 10.1016/j.immuni.2013.08.036. [PubMed: 24120362]

5. Cui W & Mehta P Identifying feasible operating regimes for early T-cell recognition: The speed, energy, accuracy trade-off in kinetic proofreading and adaptive sorting. PLoS ONE 13, e0202331 (2018). doi: 10.1371/journal.pone.0202331. [PubMed: 30114236]
6. McKeithan TW Kinetic proofreading in T-cell receptor signal transduction. Proc. Natl. Acad. Sci. U. S. A 92, 5042–5046 (1995). https://www.ncbi.nlm.nih.gov/pubmed/7761445 [PubMed: 7761445]
7. Dustin ML Stop and go traffic to tune T cell responses. Immunity 21, 305–314 (2004). doi: 10.1016/j.immuni.2004.08.016. [PubMed: 15357942]
8. Lo WL & Allen PM Self-peptides in TCR repertoire selection and peripheral T cell function. Curr. Top. Microbiol. Immunol 373, 49–67 (2014). doi: 10.1007/82_2013_319. [PubMed: 23612987]
9. Siller-Farfan JA & Dushek O Molecular mechanisms of T cell sensitivity to antigen. Immunol. Rev 285, 194–205 (2018). doi: 10.1111/imr.12690. [PubMed: 30129204]
10. Germain RN Computational analysis of T cell receptor signaling and ligand discrimination--past, present, and future. FEBS Lett 584, 4814–4822 (2010). doi: 10.1016/j.febslet.2010.10.027. [PubMed: 20965176]
11. Gaud G, Lesourne R & Love PE Regulatory mechanisms in T cell receptor signalling. Nat. Rev. Immunol, 10.1038/s41577-018-0020-8, 2018/05/24 (2018). doi: 10.1038/s41577-018-0020-8.
12. Courtney AH, Lo WL & Weiss A TCR Signaling: Mechanisms of Initiation and Propagation. Trends Biochem. Sci 43, 108–123 (2018). doi: 10.1016/j.tibs.2017.11.008. [PubMed: 29269020]
13. Balagopalan L, Kortum RL, Coussens NP, Barr VA & Samelson LE The linker for activation of T cells (LAT) signaling hub: from signaling complexes to microclusters. J. Biol. Chem 290, 26422–26429 (2015). doi: 10.1074/jbc.R115.665869. [PubMed: 26354432]
14. Andreotti AH, Schwartzberg PL, Joseph RE & Berg LJ T-cell signaling regulated by the Tec family kinase, Itk. Cold Spring Harb Perspect Biol 2, a002287 (2010). doi: 10.1101/cshperspect.a002287. [PubMed: 20519342]
15. Shah NH et al. An electrostatic selection mechanism controls sequential kinase signaling downstream of the T cell receptor. Elife 5 (2016). doi: 10.7554/eLife.20105.
16. Shah NH, Lobel M, Weiss A & Kuriyan J Fine-tuning of substrate preferences of the Src-family kinase Lck revealed through a high-throughput specificity screen. Elife 7 (2018). doi: 10.7554/eLife.35190.
17. Houtman JC, Houghtling RA, Barda-Saad M, Toda Y & Samelson LE Early phosphorylation kinetics of proteins involved in proximal TCR-mediated signaling pathways. J. Immunol 175, 2449–2458 (2005). https://www.ncbi.nlm.nih.gov/pubmed/16081816 [PubMed: 16081816]
18. Schoenborn JR, Tan YX, Zhang C, Shokat KM & Weiss A Feedback circuits monitor and adjust basal Lck-dependent events in T cell receptor signaling. Sci Signal 4, ra59 (2011). doi: 10.1126/scisignal.2001893. [PubMed: 21917715]
19. Zhang W, Sloan-Lancaster J, Kitchen J, Trible RP & Samelson LE LAT: the ZAP-70 tyrosine kinase substrate that links T cell receptor to cellular activation. Cell 92, 83–92 (1998). https://www.ncbi.nlm.nih.gov/pubmed/9489702 [PubMed: 9489702]
20. Stoica B et al. The amino-terminal Src homology 2 domain of phospholipase C gamma 1 is essential for TCR-induced tyrosine phosphorylation of phospholipase C gamma 1. J. Immunol 160, 1059–1066 (1998). https://www.ncbi.nlm.nih.gov/pubmed/9570517 [PubMed: 9570517]
21. Songyang Z et al. SH2 domains recognize specific phosphopeptide sequences. Cell 72, 767–778 (1993). https://www.ncbi.nlm.nih.gov/pubmed/7680959 [PubMed: 7680959]
22. Lo WL et al. Lck promotes Zap70-dependent LAT phosphorylation by bridging Zap70 to LAT. Nat. Immunol 19, 733–741 (2018). doi: 10.1038/s41590-018-0131-1. [PubMed: 29915297]
23. Rosette C et al. The impact of duration versus extent of TCR occupancy on T cell activation: a revision of the kinetic proofreading model. Immunity 15, 59–70 (2001). https://www.ncbi.nlm.nih.gov/pubmed/11485738 [PubMed: 11485738]
24. Hogquist KA et al. T cell receptor antagonist peptides induce positive selection. Cell 76, 17–27 (1994). https://www.ncbi.nlm.nih.gov/pubmed/8287475 [PubMed: 8287475]
25. Hogquist KA et al. Identification of a naturally occurring ligand for thymic positive selection. Immunity 6, 389–399 (1997). https://www.ncbi.nlm.nih.gov/pubmed/9133418 [PubMed: 9133418]
26. Stepanek O et al. Coreceptor scanning by the T cell receptor provides a mechanism for T cell tolerance. Cell 159, 333–345 (2014). doi: 10.1016/j.cell.2014.08.042. [PubMed: 25284152]

27. Sun S, Zhang X, Tough DF & Sprent J Type I interferon-mediated stimulation of T cells by CpG DNA. J. Exp. Med 188, 2335–2342 (1998). https://www.ncbi.nlm.nih.gov/pubmed/9858519 [PubMed: 9858519]
28. Shen S, Zhu M, Lau J, Chuck M & Zhang W The essential role of LAT in thymocyte development during transition from the double-positive to single-positive stage. J. Immunol 182, 5596–5604 (2009). doi: 10.4049/jimmunol.0803170. [PubMed: 19380807]
29. Donnelly ML et al. Analysis of the aphthovirus 2A/2B polyprotein 'cleavage' mechanism indicates not a proteolytic reaction, but a novel translational effect: a putative ribosomal 'skip'. J. Gen. Virol 82, 1013–1025 (2001). doi: 10.1099/0022-1317-82-5-1013. [PubMed: 11297676]
30. Covacu R et al. System-wide Analysis of the T Cell Response. Cell Rep 14, 2733–2744 (2016). doi: 10.1016/j.celrep.2016.02.056. [PubMed: 26972015]
31. Flajnik MF A cold-blooded view of adaptive immunity. Nat. Rev. Immunol 18, 438–453 (2018). doi: 10.1038/s41577-018-0003-9. [PubMed: 29556016]
32. Conrad ML, Davis WC & Koop BF TCR and CD3 antibody cross-reactivity in 44 species. Cytometry A 71, 925–933 (2007). doi: 10.1002/cyto.a.20435. [PubMed: 17654651]
33. Weiss A, Shields R, Newton M, Manger B & Imboden J Ligand-receptor interactions required for commitment to the activation of the interleukin 2 gene. J. Immunol 138, 2169–2176 (1987). https://www.ncbi.nlm.nih.gov/pubmed/3104454 [PubMed: 3104454]
34. Weiss A, Imboden J, Shoback D & Stobo J Role of T3 surface molecules in human T-cell activation: T3-dependent activation results in an increase in cytoplasmic free calcium. Proc. Natl. Acad. Sci. U. S. A 81, 4169–4173 (1984). https://www.ncbi.nlm.nih.gov/pubmed/6234599 [PubMed: 6234599]
35. Juang J et al. Peptide-MHC heterodimers show that thymic positive selection requires a more restricted set of self-peptides than negative selection. J. Exp. Med 207, 1223–1234 (2010). doi: 10.1084/jem.20092170. [PubMed: 20457759]
36. Bartelt RR & Houtman JC The adaptor protein LAT serves as an integration node for signaling pathways that drive T cell activation. Wiley Interdiscip Rev Syst Biol Med 5, 101–110 (2013). doi: 10.1002/wsbm.1194. [PubMed: 23150273]
37. Houtman JC et al. Binding specificity of multiprotein signaling complexes is determined by both cooperative interactions and affinity preferences. Biochemistry (Mosc.) 43, 4170–4178 (2004). doi: 10.1021/bi0357311.
38. Zhu M, Janssen E & Zhang W Minimal requirement of tyrosine residues of linker for activation of T cells in TCR signaling and thymocyte development. J. Immunol 170, 325–333 (2003). https://www.ncbi.nlm.nih.gov/pubmed/12496416 [PubMed: 12496416]
39. Aguado E et al. Induction of T helper type 2 immunity by a point mutation in the LAT adaptor. Science 296, 2036–2040 (2002). doi: 10.1126/science.1069057. [PubMed: 12065839]
40. Sommers CL et al. A LAT mutation that inhibits T cell development yet induces lymphoproliferation. Science 296, 2040–2043 (2002). doi: 10.1126/science.1069066. [PubMed: 12065840]
41. Kortum RL et al. A phospholipase C-gamma1-independent, RasGRP1-ERK-dependent pathway drives lymphoproliferative disease in linker for activation of T cells-Y136F mutant mice. J. Immunol 190, 147–158 (2013). doi: 10.4049/jimmunol.1201458. [PubMed: 23209318]
42. Miyaji M et al. Genetic evidence for the role of Erk activation in a lymphoproliferative disease of mice. Proc. Natl. Acad. Sci. U. S. A 106, 14502–14507 (2009). doi: 10.1073/pnas.0903894106. [PubMed: 19667175]
43. Lin J & Weiss A Identification of the minimal tyrosine residues required for linker for activation of T cell function. J. Biol. Chem 276, 29588–29595 (2001). doi: 10.1074/jbc.M102221200. [PubMed: 11395491]
44. Zhang W et al. Association of Grb2, Gads, and phospholipase C-gamma 1 with phosphorylated LAT tyrosine residues. Effect of LAT tyrosine mutations on T cell angigen receptor-mediated signaling. J. Biol. Chem 275, 23355–23361 (2000). doi: 10.1074/jbc.M000404200. [PubMed: 10811803]
45. Yousefi OS et al. Optogenetic control shows that kinetic proofreading regulates the activity of the T cell receptor. Elife 8 (2019). doi: 10.7554/eLife.42475.

46. Tischer DK & Weiner OD Light-based tuning of ligand half-life supports kinetic proofreading model of T cell signaling. Elife **8** (2019). doi: 10.7554/eLife.42498.**8**

47. Tang MA, Motoshima H & Watanabe K Cold adaptation: structural and functional characterizations of psychrophilic and mesophilic acetate kinase. Protein J 33, 313–322 (2014). doi: 10.1007/s10930-014-9562-1. [PubMed: 24801996]

48. Saavedra HG, Wrabl JO, Anderson JA, Li J & Hilser VJ Dynamic allostery can drive cold adaptation in enzymes. Nature 558, 324–328 (2018). doi: 10.1038/s41586-018-0183-2. [PubMed: 29875414]

49. Flajnik MF & Kasahara M Origin and evolution of the adaptive immune system: genetic events and selective pressures. Nat. Rev. Genet 11, 47–59 (2010). doi: 10.1038/nrg2703. [PubMed: 19997068]

50. Hirano M, Das S, Guo P & Cooper MD The evolution of adaptive immunity in vertebrates. Adv. Immunol 109, 125–157 (2011). doi: 10.1016/B978-0-12-387664-5.00004-2. [PubMed: 21569914]

METHODS-ONLY REFERENCE

51. Pelosi M et al. Tyrosine 319 in the interdomain B of ZAP-70 is a binding site for the Src homology 2 domain of Lck. J. Biol. Chem 274, 14229–14237 (1999). https://www.ncbi.nlm.nih.gov/pubmed/10318843 [PubMed: 10318843]

52. Thill PA, Weiss A & Chakraborty AK Phosphorylation of a Tyrosine Residue on Zap70 by Lck and Its Subsequent Binding via an SH2 Domain May Be a Key Gatekeeper of T Cell Receptor Signaling In Vivo. Mol. Cell. Biol 36, 2396–2402 (2016). doi: 10.1128/MCB.00165-16. [PubMed: 27354065]

53. Lo WL, Solomon BD, Donermeyer DL, Hsieh CS & Allen PM T cell immunodominance is dictated by the positively selecting self-peptide. Elife 3, e01457 (2014). doi: 10.7554/eLife.01457. [PubMed: 24424413]

54. Sayers EW et al. Database resources of the National Center for Biotechnology Information. Nucleic Acids Res 37, D5–15 (2009). doi: 10.1093/nar/gkn741. [PubMed: 18940862]

55. Langenau DM et al. In vivo tracking of T cell development, ablation, and engraftment in transgenic zebrafish. Proc. Natl. Acad. Sci. U. S. A 101, 7369–7374 (2004). doi: 10.1073/pnas.0402248101. [PubMed: 15123839]

56. Altschul SF, Gish W, Miller W, Myers EW & Lipman DJ Basic local alignment search tool. J. Mol. Biol 215, 403–410 (1990). doi: 10.1016/S0022-2836(05)80360-2. [PubMed: 2231712]

57. Pruitt KD, Tatusova T & Maglott DR NCBI Reference Sequence (RefSeq): a curated non-redundant sequence database of genomes, transcripts and proteins. Nucleic Acids Res 33, D501–504 (2005). doi: 10.1093/nar/gki025. [PubMed: 15608248]

58. Crooks GE, Hon G, Chandonia JM & Brenner SE WebLogo: a sequence logo generator. Genome Res 14, 1188–1190 (2004). doi: 10.1101/gr.849004. [PubMed: 15173120]

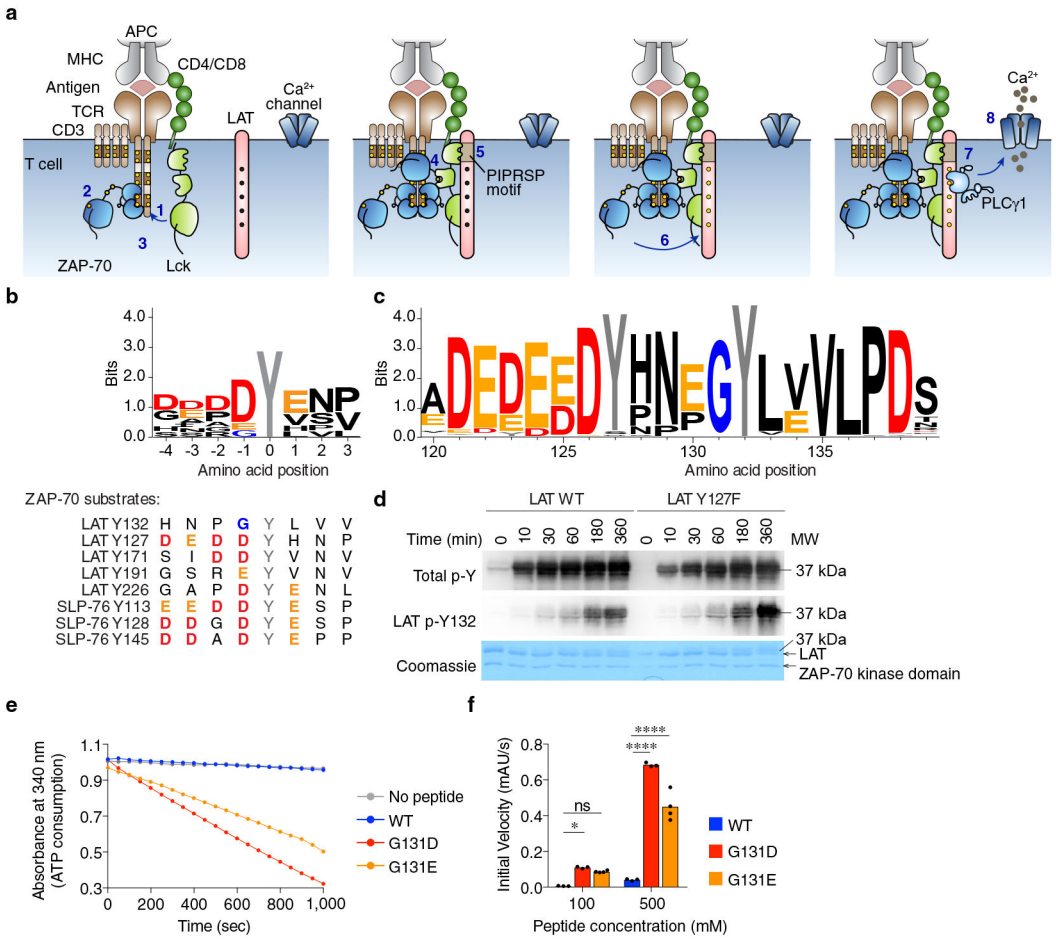

Figure 1: Mammalian LAT has a glycine preceding Y132 that decreases the phosphorylation efficiency of Y132.

a. An illustration of TCR proximal signaling after TCR:pMHC engagement. Step 1, TCR:pMHC engagement colocalizes the coreceptor-associated Lck with the pMHC stimulated TCR where Lck phosphorylates tyrosines on ITAMs of the CD3 and ζ-chains. Step 2, ZAP-70 is recruited and bound to doubly-phosphorylated ITAMs. Step 3, Lck phosphorylates ZAP-70 stabilizing its open conformation and activating the ZAP-70 catalytic domain. Step 4, Lck SH2 domain binds to ZAP-70 p-Y319, stabilizing Lck's open conformation[51, 52]. Step 5, Lck SH3 domain binds to the PIPRSP motif of LAT to facilitate the accessibility of LAT to the kinase ZAP-70[53]. Step 6, activated ZAP-70 phosphorylates tyrosines on LAT or SLP-76 (SLP-76 not shown). Step 7, phosphorylated LAT Y132 recruits PLC-γ1, leading to ITK mediate PLC-γ1 phosphorylation and activation. Step 8, activated PLC-γ1 induces calcium increase and PKC and Ras/MAPK activation (not shown), eventually leading to T cell activation.

b. Sequence logo (top) and individual sequences (bottom) showing the conservation of amino acids spanning the target tyrosines of reported ZAP-70 substrates in humans. The tyrosine substrate of ZAP-70 is referred as position 0, whereas the preceding residue is position −1.

c. Sequence conservation of LAT in 68 mammalian species, depicted in the regions surrounding tyrosines Y127 and Y132 of LAT. The amino acid position is numbered on the basis of human LAT isoform 2.

d. Immunoblot analysis of *in vitro* LAT phosphorylation reactions, monitoring site-specific phosphorylation at Y132 as well as total tyrosine phosphorylation. Purified LAT or a Y127F mutant cytoplasmic domain (5 μM) were phosphorylated by purified ZAP-70 kinase domain (1 μM). The phosphorylation of Y132 on LAT was assessed using an anti-LAT p-Y132 antibody. The total phosphorylation level of LAT is assessed using an anti-p-Y antibody (clone 4G10). A Coomassie Blue-stained membrane below shows loading levels. Data are representative of three independent experiments.

e. Phosphorylation of peptides spanning LAT Y132 with the wild-type glycine 131 residue, the G131D mutation, or the G131E mutation, using a colorimetric assay in which ATP consumption is enzymatically coupled to stoichiometric oxidation of NADH, with concomitant loss of NADH absorbance at 340 nm. The ZAP-70 kinase domain was used at a concentration of 1 μM and peptides were at a concentration of 500 μM. A control reaction lacking substrate peptide was also carried out, to measure the background level of kinase-mediated ATP hydrolysis. At least three experiments were repeated independently with similar results.

f. Background-subtracted rates of *in vitro* LAT Y132 phosphorylation using the assay described in panel (**e**). Bar graphs show the mean rate from at least three independent experiments for each kinase-substrate pair at two substrate concentrations. Each symbol represents an individual result. $n = 3$ independent results (WT and G131D); $n = 4$ independent results (G131E). *$P = 0.0389$; ****$P < 0.0001$; ns, not significant; one-way ANOVA analysis.

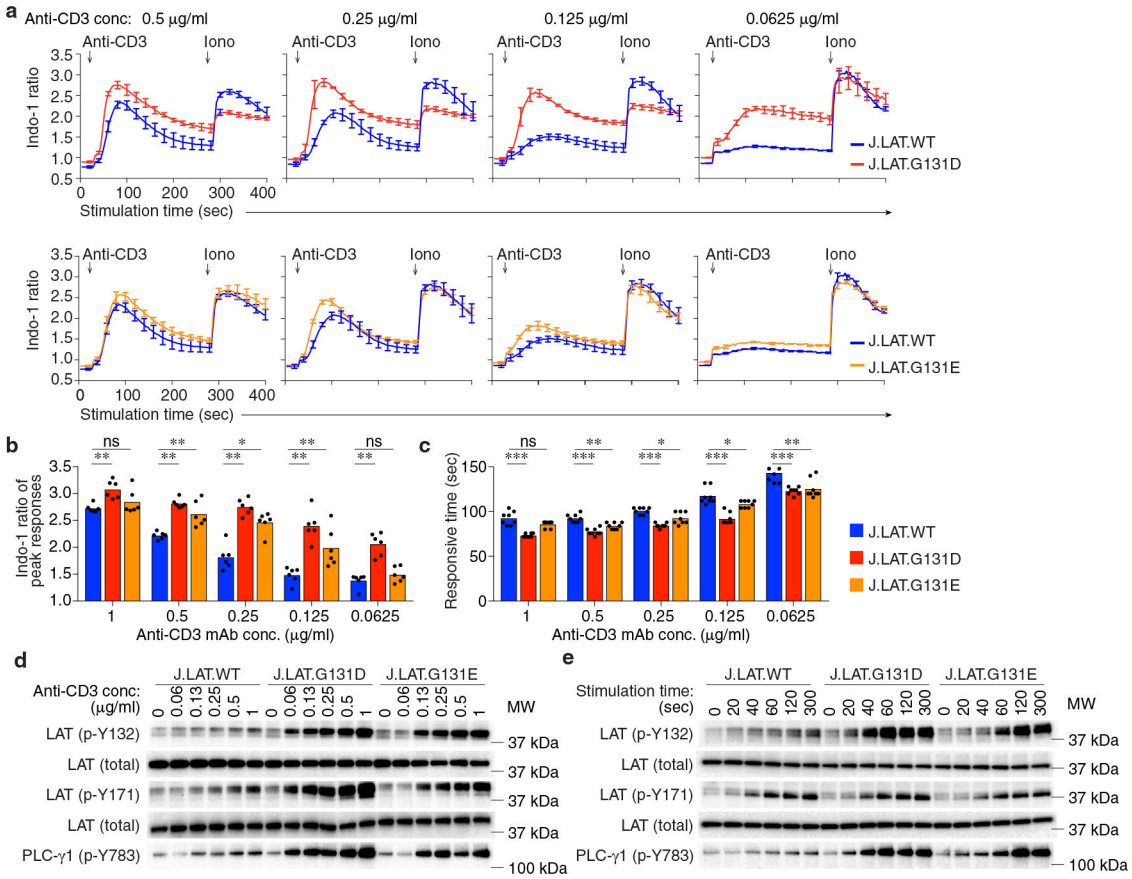

Figure 2: Mutation of LAT G131 to an aspartate or glutamate facilitates calcium responses by augmenting PLC-γ1 signaling.

a. CRISPR-Cas9-generated LAT-deficient J.LAT cells were reconstituted with wild-type LAT or mutant LAT with G131D (top) or G131E (bottom) substitutions, as indicated. Cells were loaded with the calcium-sensitive dye Indo-1 AM and stimulated with a range of anti-CD3 antibody (clone OKT3) concentration starting at 0.5 µg/ml (left) followed by a series of two-fold dilutions (0.25 µg/ml, 0.125 µg/ml, and 0.0625 µg/ml; from left to right). The changes in relative calcium-sensitive fluorescence ratios over time for 400 sec are shown (mean ± s.d; $n = 3$ technical replicates). Ionomycin (Iono) treatment was used as a positive control. Data are representative of at least three experiments.

b. The plot shows the mean of the maximal calcium peak at different concentrations of anti-CD3 antibody stimuli (mean ± s.d; $n = 8$ samples from three independent experiments). Diminishing amounts of anti-CD3 antibody were added, starting at 1 µg/ml, followed by a series of two-fold dilutions. Data were pooled from three independent experiments. $^{**}P = 0.0022$; $^{*}P = 0.0043$; ns, not significant ($P = 0.1327$). Two-tailed Mann-Whitney test.

c. Bar graphs summarize the response times to reach the peak calcium increases (mean ± s.d; $n = 8$ samples from three independent experiments). The anti-CD3 antibody stimulation starts at 1 µg/ml, followed by a series of two-fold dilutions. Data were pooled from three independent experiments. $^{***}P = 0.0002$; ns, not significant ($P = 0.3095$); $^{**}P = 0.0031$; $^{*}P$ (left) = 0.0123; $^{*}P$ (right) = 0.0228; $^{**}P$ (right) = 0.0053. Two-tailed Mann-Whitney test.

d. Immunoblot analyses of J.LAT cells that were reconstituted with wild-type LAT, G131D or G131E mutant LATs, and were left unstimulated or were stimulated with a range of anti-CD3 doses (clone OKT3) starting at 0.5 μg/ml with serial two-fold dilutions at 37°C for one minute. Data are representative of at least five experiments. Note the same lysates were run on two separate gels to blot for p-Y171 and p-Y132; hence, blots for LAT loading are provided twice.

e. Immunoblot analyses of J.LAT cells that were reconstituted with wild-type LAT, G131D or G131E mutant LATs, and were left unstimulated or were stimulated with anti-CD3 stimulation at 1 μg/ml (clone OKT3) at 37°C for different durations of time (as indicated above the blots). Data are representative of at least five experiments. Note the same lysates were run on two separate gels to blot for p-Y171 and p-Y132; hence, blots for LAT loading are provided twice.

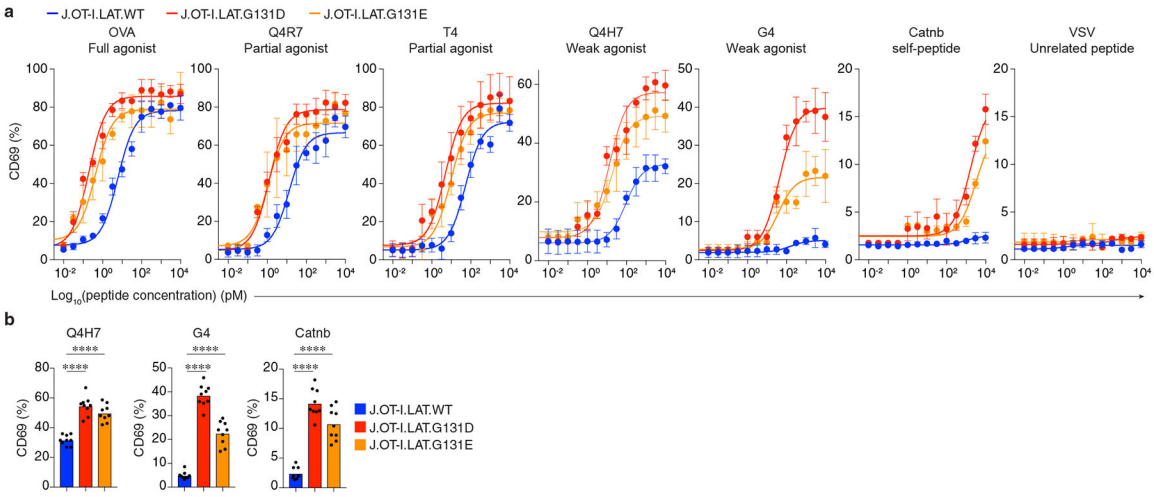

Figure 3: Enhanced Y132 phosphorylation allows T cells to react with low affinity ligands.

a. LAT-deficient J.OT-I.hCD8^{+} Jurkat variants were reconstituted with wild-type LAT, G131D or G131E mutant LATs. Cells were stimulated with T2-K^{b} antigen-presenting cells pulsed with OVA peptide, OVA APL peptides, self-peptide Catnb, or VSV control peptide over a wide range of peptide concentrations. The next day, the expression of CD69 was assessed by flow cytometry. Percentages of CD69^{+} cells were plotted against peptide concentrations (mean ± s.d; n = 3 technical replicates). Data are representative of at least five experiments.

b. Bar graph depicts the mean percentages of CD69^{+} cells after stimulation with Q4H7, G4 or Catnb peptides. Each symbol represents the result of a technical replicate (mean ± s.d; n = 9 samples from three independent experiments). P**** < 0.0001; two-tailed Mann-Whitney test.

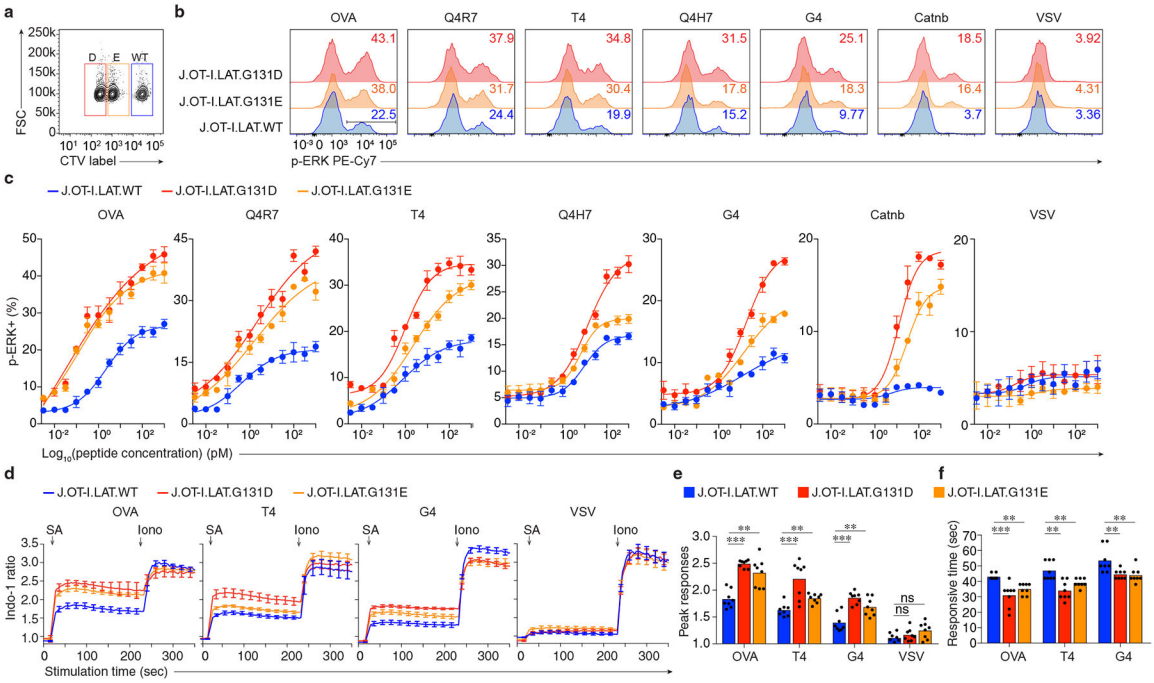

Figure 4: Substitution of G131D or G131E in LAT promotes ERK activation and calcium increase in responses to weak ligand or self-peptide stimulation.

(**a-c**) Wild-type, G131D, G131E-expressing LAT-deficient J.OT-I^{+}hCD8^{+} Jurkat variants were first individually labeled with CellTrace Violet dye at different concentrations. Cells were washed and pooled together for the experiments. T2-K^{b} cells were pulsed with OVA peptides, APL ligands, self-peptide Catnb, or VSV control peptide. Pooled J.OT-I^{+}hCD8^{+} Jurkat variants and peptide-pulsed T2-K^{b} cells were mixed on ice, and quickly spun down. Cells were then stimulated by moving them to 37°C for 5 min, and then fixed with 4% PFA to terminate the stimulation. Cells were then subjected to flow-cytometry based p-ERK analysis. Data are representative of four independent experiments.

a. Representative flow cytometry plot of J.OT-I^{+}hCD8^{+} Jurkat variants barcoded with titrated amounts of CellTrace Violet (CTV) dye.

b. Representative histograms for ERK phosphorylation responses in G131D, G131E, WT LAT-expressing J.OT-I^{+}hCD8^{+} Jurkat variants stimulated with T2-K^{b} cells pulsed with 1000 pM of each peptide as indicated. The black bar in the first panel depicts the gate used to define the p-ERK induced population in (**c**). Ligands used for stimulation are indicated above the plots.

c. Analysis of p-ERK^{+} population of G131D, G131E or WT LAT-expressing J.OT-I^{+}hCD8^{+} Jurkat variants stimulated with the indicated concentrations of peptide pulsed T2-K^{b} cells. Data were pooled from four independent experiments (mean ± s.d, n = 4 in four independent experiments). Ligands used for stimulation are indicated above the plots.

d. Wild-type, G131D, G131E-expressing LAT-deficient J.OT-I^{+}hCD8^{+} Jurkat variants were loaded with the calcium-sensitive dye Indo-1, and labeled with 1:100 biotinylated OVA/H-2K^{b}, T4/H-2K^{b}, G4/H-2K^{b} or VSV/H-2K^{b} monomers. Cells were then subjected to calcium mobilization assays on Flex Station II. Indo-1 ratios were first recorded for 30 sec to determine a relative baseline calcium level, followed by streptavidin (SA) addition to trigger

the TCR-induced calcium response. Ionomycin (Iono) was added at the 240th sec as a positive control. Representative calcium traces are shown. Each stimulus is as indicated. Data are representative of three independent experiments. (mean ± s.d; n = 3 technical replicates).

e. Bar graphs depict the statistical analysis of the fold change of the peak. Each symbol represents a technical replicate (mean ± s.d; n = 8 samples in three independent experiments). ***P = 0.0002 (OVA); ***P = 0.0006 (T4); ***P = 0.0003 (G4); **P = 0.0047 (OVA); **P = 0.0020 (T4); **P = 0.0070 (G4); ns: not significant; P = 0.3823 (VSV, left); P = 0.0830 (VSV, right). Two-tailed Mann-Whitney test.

f. Bar graphs depict the statistical analysis of the response time to reach the peak (mean ± s.d; n = 8 samples in three independent experiments). Each symbol represents a technical replicate. ***P = 0.0002 (OVA); **P = 0.0011 (OVA); **P = 0.0054 (T4, top); **P = 0.0023 (T4, bottom); **P = 0.0059 (G4, top); **P = 0.0076 (G4, bottom). Two-tailed Mann-Whitney test.

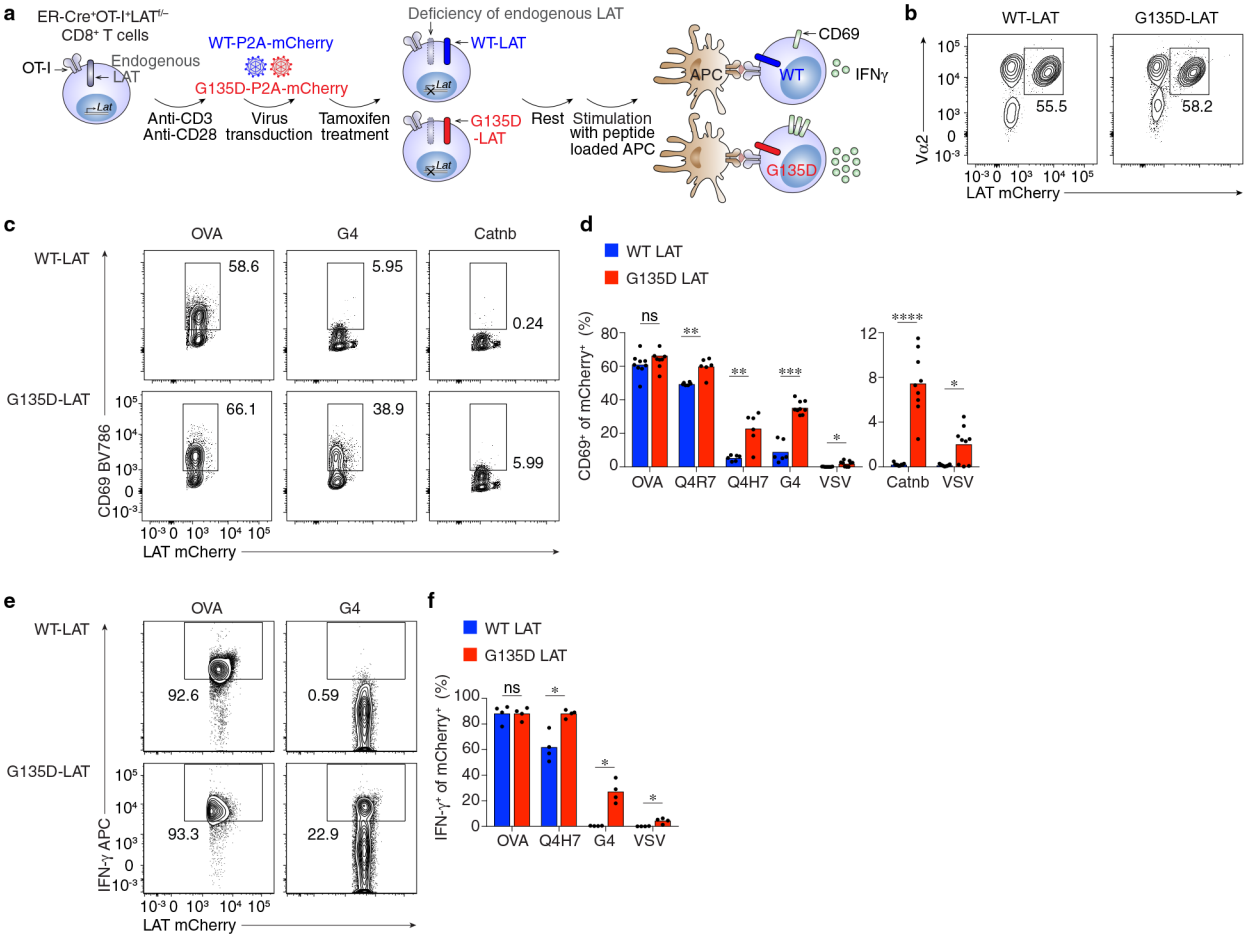

Figure 5: The G135D mutation in LAT promotes primary mouse T cells to respond to low affinity antigen or self-peptide stimulation.

a. The diagram shows the experimental flow. Naive ERCre^{+}.OT-I^{+}.LAT$^{f/-}$ CD8 T cells were isolated and lentivirally transduced to express wild-type LAT or G135D LAT and tamoxifen-treated for 4 days to delete endogenous LAT. Mouse G135D is homologous to human G131D. The wild-type or G135D LAT was conjugated to mCherry fluorescent protein through a self-cleaving P2A peptide. Cells with successful tamoxifen-induced deletion of endogenous LAT are GFP^{+} (efficiency > 90%). Cells were rested for 1 day and stimulated with peptide-pulsed TCR Cα-deficient splenocytes overnight. TCR Cα-deficient splenocytes were pulsed with 1 μM of OVA, T4, or G4 peptide, or 10 μM of Catnb peptide, or 10 μM of VSV peptide. Cells were then analyzed for their ability to upregulate CD69 and produce IFN-γ.

b. Representative contour plots depict the expression of Vα2 (OT-I TCR α chain) and mCherry after cells were transduced with lentivirus expressing wild-type LAT-P2A-mCherry or G135D LAT-P2A-mCherry. Data are representative of three experiments.

c. Flow cytometric analysis of CD69 expression in mCherry^{+} subpopulations of GFP^{+}Vα2^{+}CD8^{+} T cells, pulsed with OVA peptide, G4 peptide, or Catnb self-peptide.

d. Bar graphs represent the mean of CD69^{+} cells in the peptide stimulation assay. Each symbol represents one technical replicate (mean ± s.d; n = 9 samples in three independent

experiments). ** $P = 0.0043$ (Q4R7); ** $P = 0.0022$ (Q4H7); *** = 0.0004; **** $P < 0.0001$ (Catnb); * $P = 0.0294$ (VSV). ns: not significant; $P = 0.1359$; Two-tailed Mann-Whitney test.

e. Flow cytometric analysis of IFN-γ-producing ability in $mCherry^+$ subpopulations of $GFP^+V\alpha2^+CD8^+$ T cells, pulsed with various peptides.

f. Bar graph demonstrates the mean of IFN-γ-producing cells in the peptide stimulation assay. Each symbol represents one technical replicate. (mean ± s.d; n = 4 samples in two independent experiments.) * $P = 0.0286$; ns = not significant ($P = 0.8857$). Two-tailed Mann-Whitney test.

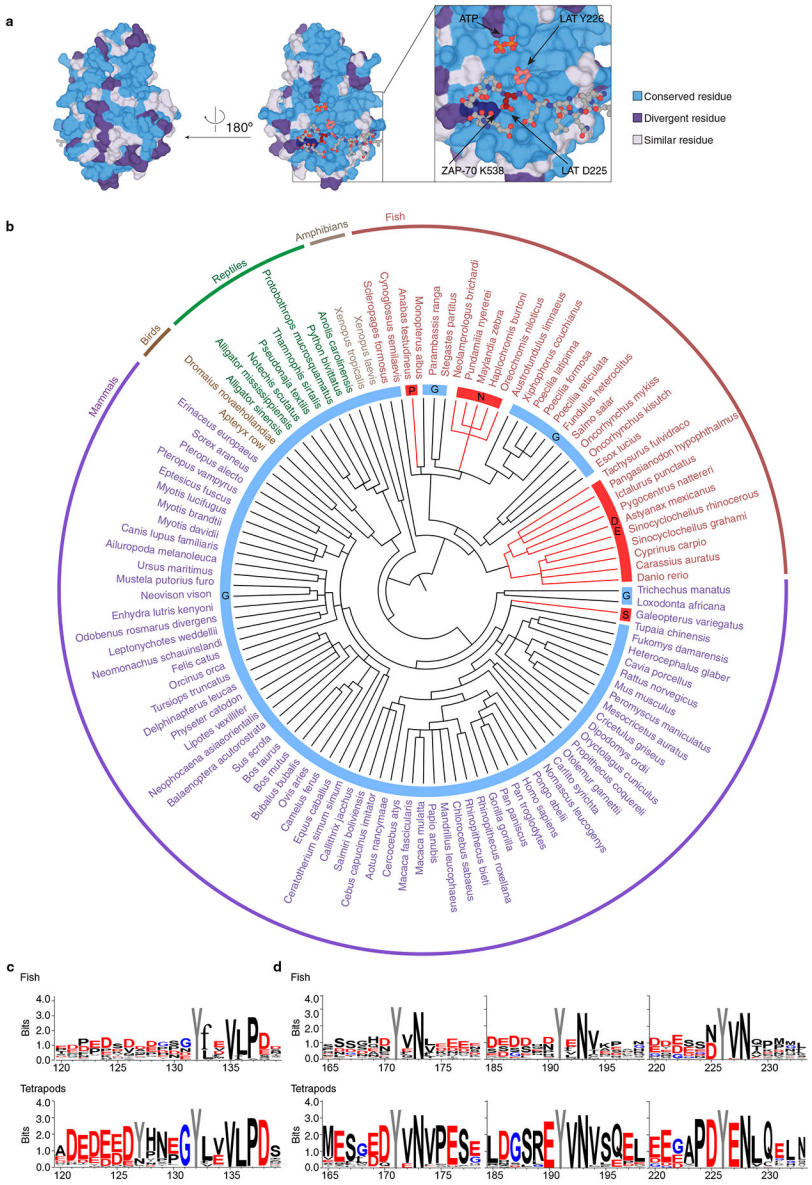

Figure 6: LAT Y132 likely represents a conserved kinetic proofreading step in tetrapodal T cells.

a. Sequence conservation between the human and zebrafish ZAP-70 kinase domains. The kinase domains of human and zebrafish ZAP-70 are 65% identical. Conservation is mapped onto a model of the human ZAP-70 kinase domain bound to a peptide surrounding LAT Y226[15]. The surface of the kinase domain is colored based which residues are identical (blue), have physiochemical similarity (light purple), or are unconserved (purple), between the human and zebrafish sequences. The peptide is shown in ball and stick representation, with LAT Y226 and the −1 residue (D225) shown in red. The conserved ZAP-70 active site residue that coordinates LAT D225, K538, is shown in dark blue. Residues in the substrate-binding region, particularly those that contact the −1 substrate residue, are highly conserved between human and zebrafish sequences, suggesting that these orthologs are likely to have similar substrate specificities.

b. Phylogenetic tree showing taxonomic relationships between various jawed vertebrate species, highlighting those species with a non-glycine residue at position 131 in LAT. Relationships are derived from the NCBI Taxonomy dataset[54]. Species that do not have glycine residue preceding Y132 in LAT are highlighted in red. These species typically have an aspartate, glutamate, asparagine, proline, or serine residue at the −1 position as indicated in the inner circle. Note that LAT sequences were not readily identifiable in most bird species, aside from emu (*Dromaius movaehollandiae*) and kiwi (*Apteryx rowi*), suggesting possible loss of the canonical jawed-vertebrate LAT gene in most birds. More details could be found in Supplementary Table 1. **c.** Sequence conservation of regions flanking LAT Y132 among fish and tetrapods. The positions are numbered using human LAT isoform 2 as a reference.

d. Sequence logo of amino acid conservation in the regions of LAT spanning Y171, Y191, or Y226. The positions are numbered using human LAT isoform 2 as a reference. Sequence conservation in fish (top) or tetrapods (bottom) is shown.

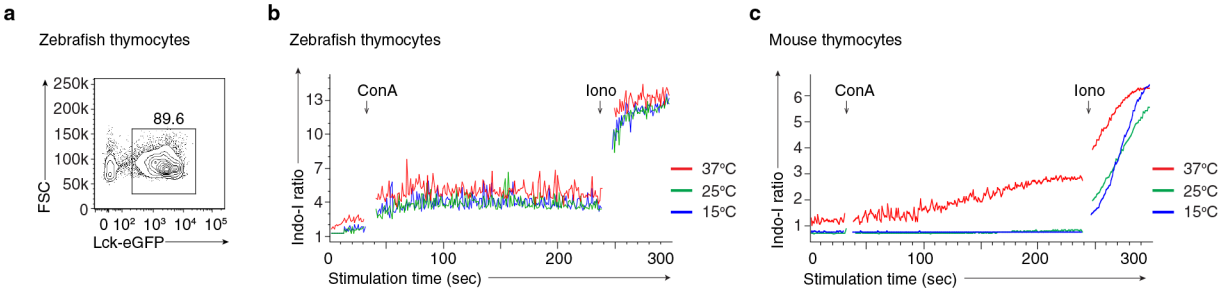

Figure 7: Cold temperature does not impair the ability of zebrafish thymocytes to trigger calcium flux in response to stimulation.

a. Representative contour plot of *lck-egfp* transgene zebrafish thymocytes. Data are representative of at least three experiments.

b. Representative calcium flux of Lck-eGFP^{+} zebrafish thymocytes treated with 10 μg/ml Concanavalin A (Con A). Zebrafish thymocytes were loaded with the calcium indicator dye Indo-1, and incubated at 25°C, 37°C or 15°C before being used for experiments. Con A was added at the 30th sec and ionomycin (Iono) was added at the 240th sec. Data are representative of three independent experiments.

c. Representative calcium responses of mouse thymocytes treated with 10 μg/ml Con A. Mouse thymocytes were loaded with the calcium indicator dye Indo-1, and incubated at 37°C, 25°C, or 15°C before they were used for experiments. Con A was added at the 30th sec and ionomycin (Iono) was added at the 240th sec. Data are representative of two independent experiments.

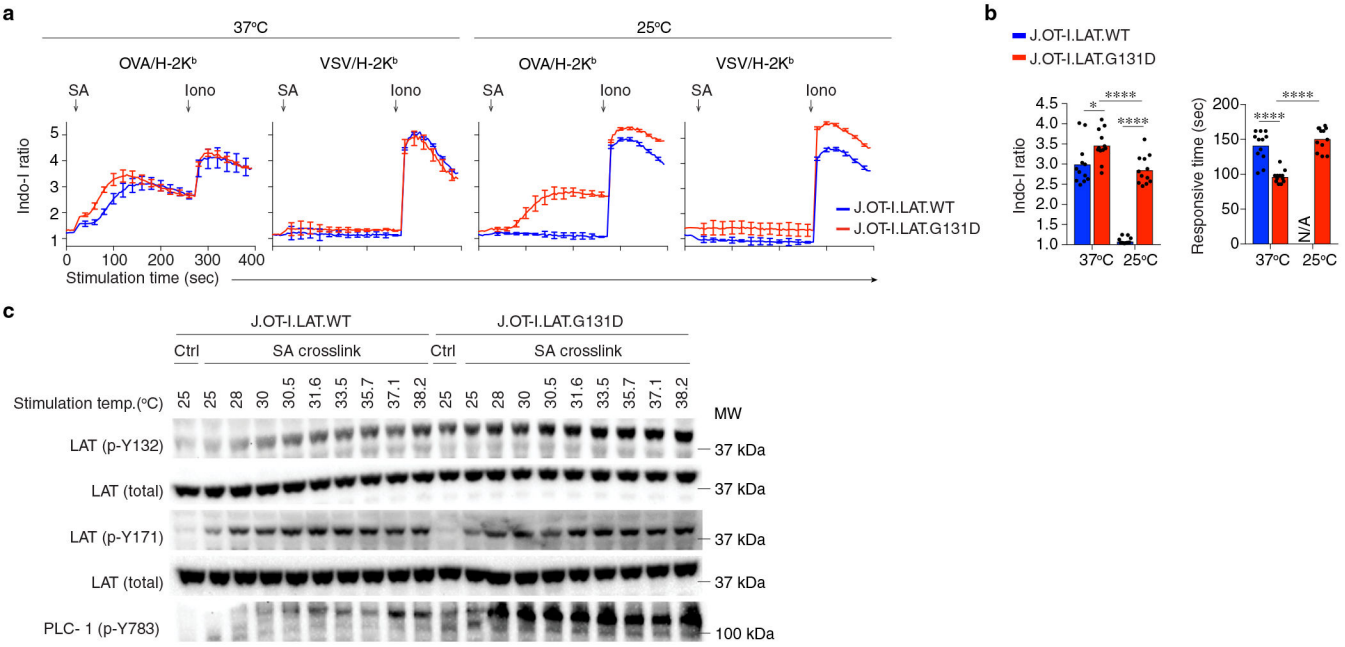

Figure 8: Expression of LAT G131D endows T cells with the zebrafish thymocyte-like ability to promote calcium mobilization at lower temperature.

a. LAT-deficient J.OT-I.hCD8^{+} cells that were reconstituted with wild-type LAT or G131D mutant LAT were used for the calcium assays. Cells were labeled with calcium-sensitive dye Indo-1, washed, and labeled with biotinylated OVA-bound I-K^{b} monomers or control VSV-bound I-K^{b} monomers at room temperature for 30 min. Cells were then used for calcium assays and stimulated by the addition of streptavidin (SA). Calcium traces were recorded for 400 sec at 37°C (left two panels) or 25°C (right two panels). Data are representative of two independent experiments. (mean ± s.d; n = 3 technical replicates.)

b. The bar graphs (left) depict the mean of the maximal calcium peak for cells at different temperatures (mean ± s.d; n = 12 samples from four independent experiments) as in (**a**). *P = 0.0145; ***P = 0.0007, ****P < 0.0001; two tailed Mann-Whitney test. Bar graphs (right) summarize the response time to reach the peak calcium responses (mean ± s.d; n = 12 technical replicates). ****P < 0.0001; two tailed Mann-Whitney test. Wild-type LAT-expressing J.OT-I^{+} cells did not respond to OVA/H-2K^{b} stimulation at 25°C, and thus were not included for analysis (labeled as N/A).

c. LAT-deficient J.OT-I.hCD8^{+} cells that were reconstituted with wild-type LAT or G131D mutant LAT were used for the experiments. Cells were labeled with biotinylated OVA-bound I-K^{b} monomers (1:100) at room temperature for 30 min. Cells were then aliquoted and transferred to PCR tubes, stimulated with the addition of streptavidin (SA), and then incubated at room temperatures (25°C), 28°C, or in PCR machine with a gradient of temperatures (30–39°C) for 10 min. The reaction was stopped by the addition of 10× lysis buffer and used for immunoblot analysis. Blots were probed with antibodies of the indicated specificities. Data are representative of at least four independent experiments.

Table 1:

Peptide	Selecting effect on thymocytes	KD by SPR	EC50			1/potency		
			WT	G131D	G131E	WT	G131D	G131E
OVA	Negative selection	54 μM	6.19	0.69	1.24	1	0.1	0.2
Q4R7	Partial	288 μM	14.92	4.23	4.27	2.7	0.6	0.7
T4	Partial/boarder	444 μM	82.67	4.89	9.34	13.8	0.7	1.5
Q4H7	Positive selection	847 μM	87.89	15.56	18.11	34.5	3.5	4.5
G4	Positive selection	>1000 μM	231.4	39.04	97.24	588.0	19.2	60.6
Catnb	Positive selection	N.A.	N.A.	1246	2116	N.A.	1090.4	2453.2

Table shows EC_{50} (pM) and ligand potency analysis of CD69 upregulation from assays as in Fig. 3a. K_D values, determined by surface plasmon resonance, were obtained from the literature[26].